Air Pollution Science for the 21st Century
J. Austin, P. Brimblecombe and W. Sturges, editors

Chapter 20

Review and intercomparison of operational methods for the determination of the mixing height

Petra Seibert[a], Frank Beyrich[b], Sven-Erik Gryning[c], Sylvain Joffre[d], Alix Rasmussen[e], Philippe Tercier[f]

[a] *Institute of Meteorology and Physics, University of Agricultural Sciences Vienna (BOKU), Türkenschanzstr. 18, A-1180 Wien, Austria*
E-mail: seibert@boku.ac.at

[b] *Meteorologisches Observatorium Lindenberg, Deutscher Wetterdienst, D-15864 Lindenberg, Germany*
E-mail: frank.beyrich@dwd.de

[c] *Meteorology and Wind Energy Department, Risø National Laboratory, DK-4000 Roskilde, Denmark*
E-mail: sven-erik.gryning@risoe.dk

[d] *Finnish Meteorological Institute, P.B. 503, FIN-00101 Helsinki, Finland*
E-mail: sylvain.joffre@fmi.fi

[e] *Danish Meteorological Institute, Lyngbyvej 100, DK-2100 Copenhagen, Denmark*
E-mail: ali@dmi.min.dk

[f] *Swiss Meteorological Institute, Les Invuardes, CH-1530 Payerne, Switzerland*
E-mail: pht@sap.sma.ch

Abstract

The height of the atmospheric boundary layer (ABL) or the mixing height (MH) is a fundamental parameter characterising the structure of the lower troposphere. Two basic possibilities for the practical determination of the MH are its derivation from profile data (measurements or numerical model output) and its parameterisation using simple equations or models (which only need a few measured input values). Different methods suggested in the literature are reviewed in this paper. The most important methods have been tested on data sets from three different sites in Europe (Cabauw – NL, Payerne – CH, Melpitz – D). Parcel and Richardson number methods applied to radiosonde profiles and the analysis of sodar and wind profiler data have been investigated. Modules for MH determination implemented in five currently used meteorological preprocessors for dispersion models have been tested, too. Parcel methods using a revised coefficient for the excess temperature and Richardson number methods using a surface excess

First published in Atmospheric Environment 34 (2000) 1001–1027

temperature worked well under convective conditions. Under stable conditions, the inherent difficulties call for a combination of several methods (e.g., mast and sodar). All the tested parameterisation schemes showed deficiencies under certain conditions, thus requiring more flexible algorithms able to take into account changing and non-classical conditions. Recommendations are formulated regarding both the analysis of profile measurements and the use of parameterisations and simple models, and suggestions for the preprocessor development and for future research activities are presented.

1. Introduction

Air quality assessments at the local or regional scale are required for a variety of purposes, e.g., emission control, air quality forecasts and implementation of legislation, and can be carried out using different types of models. A key input to these models are the meteorological data required to compute the transport, dispersion and removal of pollutants. The dispersion of pollutants depends mostly on atmospheric turbulence, but turbulence measurements per se are not routinely performed by meteorological services. Thus, dispersion characteristics are either inferred from basic meteorological parameters such as wind, temperature and radiation using parameterisation schemes or from the output of numerical models.

On the background of increasing internationalisation of policy and trade exchange there is a need for the harmonisation of legislation (e.g., on air quality), so that assessment methods applied in different countries are transparent and comparable. As a first step in that direction, an intercomparison of meteorological preprocessors embedded in some air quality models used in Europe was conducted within the COST[1] Action 710. This action was divided into 4 working groups: surface energy balance, mixing layer height, vertical profiles of mean and turbulent quantities, and complex terrain (Fisher et al., 1998). This paper is based on the comprehensive final report of the working group dealing with the mixing layer height (Seibert et al., 1998).

2. The concept of the mixing layer and definition of its height

Substances emitted into the atmospheric boundary layer (ABL) are gradually dispersed horizontally and vertically through the action of turbulence, and finally become completely mixed over this layer if sufficient time is given and if there are no significant sinks. Therefore, it has become customary in air pollution meteorology to use the term "mixed layer" or "mixing layer". Since

[1] COST: European Co-operation in the Field of Scientific and Technological Research.

under stable conditions complete mixing is often not reached, the term "mixing layer" seems preferable, because it emphasises more the process than the result. Obviously, the mixing layer coincides with the ABL if the latter is defined as the turbulent domain of the atmosphere adjacent to the ground. However, other definitions of the ABL have also been used which may, e.g., include the domain influenced by nocturnal radiative exchange processes.

The height h of the mixing layer (the mixing height MH) is a key parameter for air pollution models. It determines the volume available for the dispersion of pollutants and is involved in many predictive and diagnostic methods and/or models to assess pollutant concentrations, and it is also an important parameter in atmospheric flow models. The MH is not measured by standard meteorological practices, and moreover, it is often a rather unspecific parameter whose definition and estimation is not straightforward.

The practical and theoretical problems associated with the determination of the MH, and sometimes even its definition, are reflected in the numerous definitions found in the literature (see Stull, 1988; Garratt, 1992; Seibert et al., 1998). It seems also that the MH definitions of different authors have to be seen in the context of the data available to them.

The definition we have adopted as a general guideline for our work is: *The mixing height is the height of the layer adjacent to the ground over which pollutants or any constituents emitted within this layer or entrained into it become vertically dispersed by convection or mechanical turbulence within a time scale of about an hour.*

In order to proceed from this general definition to practical realisations, it is necessary to consider separately the structure of the stable boundary layer (SBL) and of the convective boundary layer (CBL). For the CBL, an important feature is the entrainment layer (Gryning and Batchvarova, 1994), a zone which is not well-mixed and where turbulence intensity declines towards its top. The above definition corresponds to the top of the entrainment layer. The most widespread definition, however, is the value z_i, defined as the height where the heat flux gradient reverses its sign. It is usually applied for scaling purposes and it is the definition closest to the thermodynamical CBL height definition in a zero-order jump model (i.e., where the entrainment layer thickness is neglected). We will use here this definition, but one should be aware, e.g., in the specification of turbulence parameterisations for dispersion models, that turbulence extends beyond z_i.

The SBL can be divided into two layers: a layer of continuous turbulence and an outer layer of sporadic or intermittent turbulence. Under very stable conditions the layer of sporadic turbulence may extend to the ground. Since it is notoriously difficult to measure sporadic turbulence, and even more to develop a related scaling theory, the scaling height, h, used for the SBL generally is the

layer of continuous turbulence. As in the convective case, however, this does not mean that turbulence is strictly confined to the region below h.

The asymptotic case with the heat flux approaching zero from either stable or unstable stratification is often termed neutral boundary layer. It must be kept in mind, however, that even in this case stable stratification will prevail above the ABL, which limits the validitiy of idealised concepts based on an infinitely deep neutral boundary layer. In this situation, like in the stable boundary layer, wind shear is the main source of turbulence and therefore in this paper it is subsumed under the SBL.

There are situations where these definitions have to be carefully discussed and possibly modified, e.g., patches of sporadic turbulence caused by the breaking of gravity waves, regions of turbulence generated by wind shear due to low-level jets, situations with strong non-stationarity (e.g., the evening transition period), the presence of clouds (e.g., cloud venting of the CBL, or in frontal zones), situations with significant horizontal advection, and in complex terrain regions.

We encourage researchers to pay attention to which definitions of the MH or ABL height their work is based upon, and to specify it clearly.

3. Methods for the determination of the mixing height

This section contains a literature review of practical methods for the determination of the MH. At first, we describe methods based on profile measurements and assess existing comparisons among them (Section 3.1). Then we discuss methods based on parameterisations and simple models which require only operationally available input data, from measurements or from numerical weather prediction (NWP) models (Section 3.2).

3.1. Mixing height determination from profile measurements

3.1.1. Radiosoundings

Radiosoundings are the most common source of data for operational determination of the MH. They are widely distributed, and the data are continuously quality controlled. On the other hand, at most stations they are only taken twice daily at specified synoptic times (00 UTC, 12 UTC). Consequently, in Europe the soundings can often be used as a reference for comparison with modelled MHs only around midnight and noon. Other limitations of radiosoundings are the poor vertical resolution of standard aerological data with respect to boundary layer studies, the smoothing due to the sensor lag constant bounded with

the high ascent rate of the sonde, and the fact that a sounding gives only a "snapshot"-view of the ABL structure.

MH estimations based on (standard) radiosonde data may result in quite high uncertainty (e.g., Russell et al., 1974; Hanna et al., 1985; Martin et al., 1988). Specific problems occur in the stable (nocturnal) boundary layer since no universal relationship seems to exist between the profiles of temperature, humidity or wind and turbulence parameters (heat or momentum fluxes, turbulent kinetic energy TKE). The interpretation of profiles thus is not straightforward and several criteria have been used (see Table 1 in Seibert et al., 1998).

MH estimation from profiles obtained with tethered balloons or aircraft, which may include turbulence and/or trace gas concentration profiles, is, in principle, not very different from the analysis of radiosonde data. The operation of both systems, however, is very expensive and therefore is not suited for routine applications. Temperature (and trace gas) profiles taken by commercial aircraft during take-off and landing may become a useful data source in the future.

3.1.1.1. Subjective methods. Radiosonde temperature and wind profiles in the lower part of the atmosphere are often used for a subjective estimation of the MH. Under convective conditions, the MH is often identified with the base of an elevated inversion or stable layer, or as the height of a significant reduction in air moisture, often accompanied by wind shear. Some authors recommend to take the inversion base altitude increased by half of the depth of the inversion layer as the characteristic CBL height (Stull, 1988).

3.1.1.2. Objective methods. Holzworth (1964, 1967, 1972) and others have developed objective methods to simplify and homogenise the estimation of the MH under convective conditions. The basic idea of the "Holzworth" or "parcel method" is to follow the dry adiabate starting at the surface with the measured or expected (maximum) temperature up to its intersection with the temperature profile from the most recent radiosounding. It determines the MH as the equilibrium level of a hypothetical rising parcel of air representing a thermal. However, this method strongly depends on the surface temperature, and a high uncertainty in the estimated MH value may result in situations without a pronounced inversion at the CBL top. Some authors have noticed that the MH determined by the "Holzworth method" is not strongly correlated with observed trace gas concentrations (e.g., Aron, 1983; Jones, 1985).

Different refinements of this simple scheme have been suggested, to account for temperature advection, subsidence and other effects (e.g., Miller, 1967; Garrett, 1981). They differ in how the temperature of this air parcel is found, and in the thermodynamical variable used to define the equilibrium level. An advanced parcel method has been proposed by Beljaars and Betts

Table 1. Measuring platforms and their qualification for MH determination

Method	Advantages	Shortcomings
Direct measuring techniques/sensor platforms		
Radiosonde	• Routine ascents for many years all over the world, therefore especially suited for climatological studies • Measured data transmitted via international communication networks with very short time delay, therefore well suited for operational use • Compatibility with measurements in the free atmosphere	• Crossing the ABL along a slanted path within a few minutes, provides a "snapshot"-like profile • Limited height resolution of routine ascents • Operationally only 2–4 soundings per day at fixed times, even during field campaigns 1.5–3 h as closest interval • Tracking problems at low levels (site-dependent) may affect wind profiles
Tethered balloon	• Ascent velocity can be chosen according to the desired vertical resolution • Turbulence and trace gas concentration measurements possible	• Limited to field campaigns, no unmanned operation • Synchronous profile measurement difficult • Limited measurement range, usually below 500 m • Not possible in cases of high wind speed or strong convection
Mast	• Installation of a large number of different sensor types possible including detailed turbulence measurements • Continuous operation • Good resolution of the lowest layers	• Very high installation/operation costs, increasing with height • Limited range: 50 to at most 300 m • High vertical resolution requires a high number of sensors (increasing costs)
Aircraft and remote sensing techniques		
Aircraft	• Possibility to operate many different sensors, including mean meteorology, chemistry, and turbulence sensors, as well as remote sensing systems • Provides spatial information, well suited for mesoscale studies	• High costs, only for field campaigns • Operation mostly limited to daylight hours • Lowest flight level subject to restrictions (security)
Doppler weather radar/wind profiler	• Ground based and aircraft based operation possible (for radar only) • Alternating RHI/PPI-Scan for 3D-studies (for radar only) • High sampling rate and continuous operation	• Lowest range normally not below 200 m • Limited vertical resolution (50–250 m) • Expensive • Weather radars do not work well in clear air • Interpretation not always straightforward

Table 1. (Continued)

Method	Advantages	Shortcomings
Lidar	• Ground-based and aircraft-based operation possible • Alternating RHI/PPI-Scan for 3D-studies • High sampling rate • Return signals originate directly from aerosols ("pollution")	• Expensive • Unattended operation often not possible for safety reasons • Limited range resolution and lowest range gate • Tracer necessary (gas, aerosol) • Interpretation sometimes ambiguous
Sodar	• Relatively simple, not very expensive: suited for unmanned long-term operation • High temporal and vertical resolution • Minisodars allow probing of shallow SBL	• Limited sounding range (500–1000 m) • Sensitivity to environmental noise • Noise contamination to the environment • Interpretation requires experience, sometimes ambiguous

(1992) and has been also applied (with slightly different values of the constants) by Wotawa et al. (1996) and in this paper (see Section 4.1).

Another popular approach are the bulk Richardson number methods (e.g., Troen and Mahrt, 1986; Vogelezang and Holtslag, 1996). They differ mainly in the choice of the level for the near-surface temperature and wind, the parameterisation of shear production of turbulence in the surface layer, and the consideration of an excess surface temperature under convective conditions. Parcel methods can be understood as a simplification of the Ri-number methods where the shear contribution is neglected. Thus they are only suited for unstable conditions.

Methods based on conserved variables (e.g., mixing ratio, equivalent-potential temperature, etc.) permit analyses of air mass structures and vertical mixing. Betts and Albrecht (1987) proposed respective criteria on the basis of averaged and smoothed profiles. For individual profiles, a refinement of these criteria is necessary to differentiate the main features from secondary stratification (e.g., Tercier et al., 1995).

3.1.2. Remote sounding systems

Remote sounding systems (lidars, sodars, RASS, wind profiling radars; see Clifford et al. (1994) for an overview) are more and more introduced into operational application. They provide an interesting alternative for MH estimations. The basic advantages of remote sounding systems are the continuous operation and that they do not cause any modification of the investigated flow.

The sodar is one of the simpler and less expensive remote sounding systems, making it well suited for routine operation. Sodar signals are scattered by temperature inhomogeneities characterised by the structure parameter of the acoustic refractive index, C_n^2. Vertical profiles of C_n^2 and thus the sodar backscatter intensity show typical features under stable and convective conditions (e.g., a strong decrease above a region of less variable C_n^2 in a SBL with significant shear-produced turbulence, or an elevated maximum at the top of a CBL) which can be used to derive the MH (for more details, see Beyrich, 1997). In addition, sodar systems with Doppler capability allow determination of the mean wind and vertical velocity variance profiles which may also be employed for MH determination. Methods and algorithms to derive the MH from sodar data are compiled in Beyrich (1997) and Seibert et al. (1998). However, the vertical range of most sodars is limited to a maximum of about 1 km, but often to only a few hundred metres. The lowest range gate of typical sodars is around 40 m. This is lower than for the other remotes sounding systems, but it can still be too high for very shallow SBLs. In this case, minisodars (Asimakopoulos et al., 1996) are an attractive option.

Lidars allow the measurement of aerosol or trace gas concentration profiles and may therefore be considered to provide direct measurements of the MH. Since the top of a convectively mixed layer is often associated with strong gradients of the aerosol content, a simple aerosol backscatter lidar seems suited to determine the convective MH. However, interpreting data from aerosol lidars is often not straightforward, because the detected aerosol layers are not always the result of ongoing vertical mixing, but may originate from advective transport or past accumulation processes (e.g., Russell et al., 1974; Coulter, 1979; Baxter, 1991; Batchvarova et al., 1999). Under stable conditions, problems in estimating the MH from lidar data can arise from the weak vertical gradients in the aerosol content. Moreover, in the evening, it usually takes some time until a sufficiently clear discontinuity in the backscatter intensity profile develops at the top of the SBL, within the previously well-mixed layer (e.g., Russell et al., 1974).

The boundary layer wind profiler seems to be a very promising device for direct and continuous measurement of the MH in a deep CBL (Angevine et al., 1994a,b; Gaynor et al., 1994; Dye et al., 1995). The backscatter intensity of the electromagnetic signal is proportional to the structure parameter of the electromagnetic refractive index C_n^2 which depends on small-scale fluctuations of the temperature and especially the moisture fields. Vertical profiles of C_n^2 usually show a maximum at the top of a well-developed CBL. However, the moisture profile is often not as well-mixed as that of temperature which may result in some ambiguity of the derived MHs. Additional problems occur in the presence of cumulus clouds, even if only shallow, in the upper part of the ABL.

Radio-acoustic sounding systems (RASS) are extensions of either sodars or radar wind profilers, providing in addition to wind and C_n^2 profiles also virtual potential temperature profiles. They appear therefore well suited for the determination of the MH with Richardson number methods, provided that temperature is retrieved with sufficient accuracy (Görsdorf and Lehman, 2000) and that range and resolution are adequate.

The combination of different remote sounding systems (e.g., sodar + wind profiler, or sodar + lidar) offers a promising way towards the direct and continuous monitoring of the evolution of the MH throughout the complete diurnal cycle (e.g., Beyrich and Görsdorf, 1995). However, the interpretation of data measured with remote sounding systems is not always straightforward. Nevertheless, this holds true also for the direct measuring systems and may (at least partially) be attributed to the general problem of MH definition as discussed in Section 2.

3.1.3. Assessment of measurement-based methods

3.1.3.1. General considerations. The variety of empiricial methods to estimate MHs requires a critical assessment of their advantages and shortcomings (summarised in Table 1) and the agreement of their results. Strictly following our definition given in Section 2, the MH should be determined by investigating the dispersion process of non-reactive tracer gases through the analysis of concentration profiles. However, vertical mixing is not the only process determining such profiles and additional measurements would be needed for a safe interpretation. The second-best choice would be turbulence profile measurements. Both types of measurements are difficult, expensive and therefore not operational. Thus, MH determination is based in most cases on profile measurements of mean meteorological variables such as wind, temperature, humidity, and refractive index. These profiles should satisfy the following conditions:

- They should cover the layer between the earth's surface and about 2–3 km above ground, considering the typical height range over which the MH varies during its annual and diurnal cycles in defined climatic regions.
- The profile measurements should be available with a time resolution of about 1 h or less in order to properly describe the evolution of the MH, especially during the morning and evening transition phases.
- The measured profiles must have a vertical resolution of about 10–30 m to avoid relative uncertainties of more than 10–20%, especially for low MHs (< 250 m).
- The measured parameters should be linked physically to the vertical mixing of pollutants.

Table 2. Critical assessment of different methods to determine the MH

	Continuous data output	Range covered well			Determination of turbulence parameters
		10–100 m (low SBL)	100–500 m (SBL/CBL)	0.5–3 km (CBL)	
In-situ measurements					
Radiosonde	.	.	✓	✓	.
Tethered balloon	.	✓	✓	.	(✓)
Mast	✓	✓	.	.	✓
Aircraft	.	.	(✓)	✓	✓
Remote Sounding					
Mini-sodar	✓	✓	.	.	✓
Sodar	✓	.	✓	.	✓
Radar[a]	✓	.	(✓)	✓	✓
RASS[b]	(✓)	.	(✓)	(✓)	(✓)
Lidar	✓	.	(✓)	✓	✓
Numer. models	(✓)	(✓)		✓	✓

Note: ✓means fulfilled; (✓) partly fulfilled and . not fulfilled.

[a]Electromagnetic boundary-layer wind profiler.

[b]As an extension of the electromagnetic boundary-layer wind profiler.

Table 2 indicates which of the above-mentioned requirements are fulfilled by the different sounding systems. It clearly appears that none of the systems meets all the requirements, i.e., the "*MH-meter*" does not exist. Reliable MH determination under all conditions is therefore still an unsolved problem. The best approach is to use a combination of systems.

In this section we discuss comparative studies of empirical MH determination. Complete agreement between MH values derived from different sounding systems cannot be expected a priori due to several reasons, the most important ones being:

- Different sounding systems measure different atmospheric parameters (mean temperature, humidity, wind, turbulent fluxes or structure parameters) with varying height resolution and accuracy.
- Vertical profiles of these parameters are influenced in a different way by the processes occurring on the earth's surface. In addition, a host of turbulent and non-turbulent processes (heating and cooling, convection and subsidence, radiation processes, baroclinity, advection, gravity waves, phase changes of water) interact with each other within the ABL and influence the vertical profiles. It is nearly impossible to separate the various contributions to the observed ABL structure.
- Often it is difficult to identify a clear upper boundary of the mixing layer or ABL because vertical profiles of turbulent parameters are smooth without any clear signatures and decrease asymptotically towards values close to

zero which are typical for the residual layer. This occurs especially under stable conditions with weak turbulence and near-neutral conditions.

3.1.3.2. Convective boundary layer. Field studies to compare MH values derived from different measurement systems (radiosonde, sodar, radar, lidar, aircraft) under convective conditions have been described, e.g., by Russell et al. (1974), Noonkester (1976), Coulter (1979), Kaimal et al. (1982), Baxter (1991) and Marsik et al. (1995). These studies show that the relative differences are mostly less than 10%, provided that the elevated inversion capping the well-mixed CBL is not too weak and has a well-defined base. Conclusions on possible systematic deviations between different estimates of the MH are not consistent (except for the lidar – see below). This should be attributed to different criteria applied to analyse the profiles as well as to the often limited number of observations and in some cases also to spatial differences between the sites where the different systems had been operated.

In cases of a weak inversion or a non-perfectly mixed CBL, measurements from different systems and even the analysis of the same potential temperature profile by several experienced meteorologists may easily result in relative differences of 25% or even larger (e.g., Hanna et al., 1985; Martin et al., 1988).

MH values derived from lidar measurements have generally been found to be slightly but systematically higher than values derived from temperature profiles or sodar measurements (e.g., Coulter, 1979; Hanna et al., 1985; Martin et al., 1988; Dupont, 1991). This is basically explained by the fact that the most energetic convective plumes penetrate into the stable or inversion layer thereby transporting aerosols up to levels higher than the mean height of the inversion or stable layer base. Under certain conditions, pollutants trapped within the stable capping inversion or free atmosphere can cause a systematic overestimation of MHs from lidar observations (McElroy and Smith, 1991).

3.1.3.3. Stable boundary layer. (a) Methods using wind and temperature profiles: The comparison of MHs derived from different observing systems under stable conditions is much more difficult. This is due to certain features of the structure and evolution of the SBL such as the intermittent and weak turbulence, gravity waves, radiative cooling, drainage flows, and inertial oscillations. Time scales of most of the relevant processes are much longer than in the CBL, so that the SBL is often far from stationarity. Different SBL height scales derived from temperature and wind profiles are compared, e.g., in Hanna (1969), Yu (1978), Mahrt and Heald (1979), Mahrt et al. (1979, 1982), Arya (1981), and Wetzel (1982). No significant relationship exists between the height scales based on the temperature profile and the height of the low-level wind maximum. This is basically due to the different time evolution of the temperature and wind profiles during the night. The surface inversion under

undisturbed meteorological conditions normally grows with time due to continuous radiative cooling (e.g., Anfossi et al., 1976; Klöppel et al., 1978; Stull, 1983a; Godowitch et al., 1985). On the contrary, the axis of the nocturnal low-level jet seems to exhibit more of a tendency to descend during the night, although the observations are sometimes contradictory (e.g., Beyrich and Klose, 1988; Mahrt et al., 1979; Godowitch et al., 1985; Smedman, 1988). Normally, a temperature-derived SBL height scale is smaller than the height of the wind maximum at the beginning of the night, whereas towards its end the opposite often holds true. Thus, the structure and the evolution stage of the SBL should be considered when deriving the stable MH from temperature or wind profiles, or when comparing MH values derived from different observing systems under stable conditions.

(b) Methods based on turbulence data: Comparing MH estimates for the SBL derived from turbulence profiles to those derived from mean temperature and wind profiles profiles is difficult due to the scarcity of data and to the variety of definitions for the SBL height. Caughey (1982) noticed that "there is no simple relationship between the SBL depth and the depth of the surface inversion layer. As this layer deepens and becomes more intense, significant turbulence exchange becomes confined to a shallow layer close to the ground". This was confirmed by Garratt (1982a) and Smedman (1991). Kurzeja et al. (1991) found a good correlation between the top of a strong surface inversion and a SBL height derived from profile measurements of the wind direction standard deviation at the beginning of the night and in general between the latter height and the height of the wind maximum. Model calculations often show an increase of the SBL height defined by the turbulence profile or a different time behaviour during different phases of the SBL evolution (e.g., Nieuwstadt and Driedonks, 1979). Model simulations using a one-dimensional ABL model with an algebraically approximated second-order closure (Dörnbrack, 1989) have shown that the turbulent MH scales derived from the vertical profiles of heat flux, momentum flux, and TKE exhibit both a different behaviour in time and a different relationship between each other, depending on the external conditions (Beyrich, 1994b). The level at which the turbulent heat flux has decreased to 5% of its surface layer value is often used as a definition of the MH under stable conditions. Mason and Derbyshire (1990) deduced from large-eddy simulations (LES) that "if radiative heat transfer is negligible, the flux of heat is roughly analogous to that of contaminants emitted from low-level sources, and so definitions of SBL depth based on the buoyancy flux profile are easy to relate to a 'mixing depth' appropriate for dispersion applications". The turbulent SBL height scale estimated from profiles by determining the level at which the gradient Richardson number Ri exceeds a critical value Ri_c, depends on the vertical resolution of the profile data used, and there is still some controversy about the numerical value of Ri_c. Thus, it is clear that

the question which of the suggested SBL height scales is best suited to characterise the vertical mixing of pollutants under stable conditions has not received yet a final answer.

(c) Methods using remote sounding data: Among the remote sounding instruments, solely acoustic sounders seems capable in providing MH data under stable conditions. Radar profilers and lidars have mostly a range resolution which does not allow to resolve the SBL in detail. In addition, their first usable range gate is often at or above the SBL top, a fact which sometimes even limits the application of a conventional sodar (Garratt, 1982b; Smedman, 1988; Baxter, 1991). For very shallow stable boundary layers (below 50–100 m), minisodars – with a lowest range gate around 10 m – can overcome this deficit. Unfortunately, the interpretation of sodar data for MH determination under stable conditions is controversial (Hanna, 1992). Results from comparisons of sodar measurements with MHs derived from temperature and wind profiles are quite inconsistent (Arya, 1981; Hanna et al., 1985). No systematic differences between sodar observations and the height of the nocturnal surface inversion were found by Hicks et al. (1977), Hayashi (1980), or Fitzharris et al. (1983). Some authors concluded that the sodar-based MH is generally lower than the surface inversion height (Nieuwstadt and Driedonks, 1979; Bacci et al., 1984). Piringer (1988) found agreement with the top of the lowest strongly stable layer of a layered surface inversion. Gland (1981) and Dohrn et al. (1982) did not find any clear connection between echo intensity and inversion features. On the other hand, the rare comparisons of sodar observations with turbulent MH scales by Nieuwstadt and Driedonks (1979) and Tjemkes and Duynkerke (1989) yielded a reasonable agreement between sodar data and the height at which modelled sensible heat flux or TKE have decreased to 5% of their surface layer values. Dupont (1991) and Devara et al. (1995) found a good agreement between MH values derived from simultaneous sodar and lidar operation, though based on a small number of case in a simply structured SBL. Van Pul et al. (1994) found a high correlation between the SBL height derived from lidar measurements and radiosonde profiles. Comparing ozone profiles measured with a tethered balloon and sodar data under conditions of a complex structured SBL, Beyrich et al. (1996) reported a generally good agreement of the MH values derived from both systems, except for very low MHs. All these findings are consistent with the fact that the sodar echo intensity is more or less strongly influenced by turbulence whereas inversion heights are also influenced by radiative cooling. Beyrich and Weill (1993) have demonstrated that the relationship between a sodar-derived value for the stable MH and any other height scale strongly depends on the stage of the SBL evolution. They concluded that different criteria have to be applied to derive a MH value from sodar signal intensity profiles depending on the actual shape of these profiles. Beyrich (1994a) demonstrated that a well-developed nocturnal low-level jet

governs the time evolution of the stable MH especially in the second half of the night.

3.2. Mixing height determination from parameterisations and models

As continuous profile measurements for the operational determination of the MH are not generally available, simple parameterisations based on standard surface observations and single profile data as well as numerical models are widely used in the practice of meteorological and environmental services. Simple diagnostic or prognostic parameterisation equations for the MH are still very attractive for operational purposes because of their simplicity and the limited number of required input data. They are also used within comprehensive parameterisation schemes for the treatment of the ABL in some numerical weather prediction and climate models.

One-dimensional prognostic models of the atmosphere with (local) turbulence closure of the order of 1.5, 2 or even higher have been used by different authors over the last 20 yr in order to estimate the height of the stable turbulent boundary layer, usually as the level where turbulence (measured by the TKE, the heat flux, or the momentum flux) decays below a certain threshold (e.g., Delage, 1974; Wyngaard, 1975; Brost and Wyngaard, 1978; Rao and Snodgrass, 1979; Nieuwstadt and Driedonks, 1979; Dörnbrack, 1989; Tjemkes and Duynkerke, 1989; Estournel and Guedalia, 1990). They could be considered an alternative to simple parameterisations, especially if coupled to observations. Over the last years, also three-dimensional numerical flow models have been increasingly used to derive MH values, and especially to produce regional MH patterns over larger areas (e.g., Sørensen and Rasmussen, 1997; Fay et al., 1997). Successful intercomparisons of daytime maximum MHs from a NWP model and observed values from windprofiler measurements over a several weeks period have been presented by Engelbart (1998). Klein Baltink and Holtslag (1997) found differences between model results and measurements up to a factor of two for the daytime maximum MHs which they attributed to a wrong soil moisture in the model. Batchvarova et al. (1999) found good agreement between a comprehensive data set on the MH in a coastal area determined from different observational devices (balloons, airborne lidar) and the MH derived from the RAMS model, where the top of the MH was identified by a critical value of the TKE. This development will certainly continue, as non-hydrostatic models with a few kilometres horizontal resolution and turbulence closures based on a prognostic equation for TKE are widespread research tools nowadays and are about to be used as operational NWP models (e.g., Schlünzen, 1994). More systematic comparisons of MHs derived from these models and from observations are desirable. It is intrinsic to them that they are prognostic, and unless four-dimensional variational data assimilation

is applied, they will not be able to make full use of existing observations. Their use is justified especially in situations with strong horizontal inhomogeneities, and if geographical fields of the MH are needed.

3.2.1. Modelling and parameterisation of the MH under stable conditions

Many parameterisation expressions for the height of the turbulent SBL have been suggested in the literature (e.g., Hanna, 1969; Zilitinkevich, 1972; Etling and Wippermann, 1975; Arya, 1981; Mahrt, 1981; Nieuwstadt, 1984; Koracin and Berkowicz, 1988). Both diagnostic and prognostic relationships have been proposed and there has been a controversial debate on which type is the most suitable (Nieuwstadt, 1981, 1984; Garratt, 1982a,b).

The most popular *diagnostic equations* (based on scaling arguments) are:

$$h = a_1 L_E = a_1 u_*/f \tag{1}$$

and

$$h = a_2 (L_E L_*)^{1/2} = \frac{a_2 u_*^2}{\sqrt{-\beta \kappa Q_0 f}} \tag{2}$$

with the empirical coefficients $a_1 = 0.07$–0.3 and $a_2 = 0.3$–0.7. Nieuwstadt (1981) proposed a combination of (1) and (2), namely:

$$h = \frac{L_*}{3.8}\left(-1 + \sqrt{1 + 2.28 \frac{u_*}{f L_*}}\right). \tag{3}$$

Most of the verification studies done in the past do not seem to favour the application of more elaborated parameterisations. However, one should be cautious in using these equations because Eq. (1) assumes a neutral, stationary boundary layer, and because $1/f$ is generally too long to be a relevant time scale. The subordinate role of the Coriolis force for the turbulent fluxes is also supported by large-eddy simulation (see Fig. 11 in Andrén, 1995).

As an alternative to $1/f$ as time scale, some authors, e.g., Kitaigorodskii and Joffre (1988), have suggested to use $1/N_{BV}$, and

$$h = a_3 L_N = a_3 \frac{u_*}{N_{BV}} \tag{4}$$

with the empirical constant $a_3 = 4$–14. This model has been corroborated by measurements in the Arctic (Overland and Davidson, 1992), by lidar measurements in the Netherlands (van Pul et al., 1994), and by LES-computations (Vogelezang and Holtslag, 1996).

Classically, it is assumed that the structure of the stable ABL depends on external parameters such as the Coriolis parameter f and the surface roughness length z_0, and on internal turbulent parameters such as the friction velocity u_* and the surface heat flux $Q_0 = \langle w'\Theta' \rangle$. Then, the stable (and neutral) ABL height is assumed to be a function of the Ekman and Monin-Obukhov length scales $L_E = u_*/f$ and $L_* = -u_*^3/(\beta \kappa Q_0)$, respectively. Joffre (1981) and Kitaigorodskii and Joffre (1988) have extended these similarity theories to include the effect of the background stratification of the atmosphere through the length scale $L_N = u_*/N_{BV}$, with the Brunt-Väisälä frequency $N_{BV} = \sqrt{\beta \gamma_\theta}$, where γ_θ is the potential temperature gradient above the MH. Zilitinkevich and Mironov (1996) have proposed a multi-asymptotic expression which combines all these different scales. A comprehensive survey of the various formulations can be found in Seibert et al. (1998).

It has also been proposed to set h proportional to L_*. A wide range of constants have been found for this relationship, between 1.2 and 100 (Zilitinkevich and Mironov, 1996); values between 2 and 10 appear to be most typical (Arya, 1981).

A second controversy has been whether it is possible to parameterise the SBL height solely based on surface layer variables (mainly u_*, L_*), or whether bulk SBL parameters should be considered additionally or even exclusively (e.g., Mahrt, 1981; Garratt, 1982b; Smedman, 1991; Vogelezang and Holtslag, 1996). Diagnostic formulae considering the bulk structure of the SBL are based on the assumption that turbulence production must vanish at the top of the SBL and the Richardson number must therefore exceed its critical value Ri_c (Hanna, 1969; Mahrt et al., 1979). Thus,

$$h = Ri_c (\Delta V)^2 / \beta \, \Delta\Theta. \tag{5}$$

The proposed equations differ basically in the choice of the levels over which the wind and temperature differences ΔV and $\Delta\Theta$ across the ABL are determined and in the value of Ri_c ($Ri_c = 0.33$, Hanna (1969), Wetzel (1982); $Ri_c = 0.5$, Mahrt (1981), Troen and Mahrt (1986); $Ri_c = 0.25$, Holtslag et al. (1990)). Joffre (1981) found that the value of Ri_c depends on the parameter hf/u_* with the classical value of 0.25 being relevant for small values of hf/u_* ($\leqslant 0.1$), but large values of $Ri_c \sim 7$ can be reached when $hf/u_* \geqslant 0.3$ (see also Maryon and Best, 1992). Vogelezang and Holtslag (1996); hereafter the VH-method) extended this method by incorporating shear production in the surface layer parameterised by an additional term depending on u_*.

Most *prognostic equations* proposed to describe the SBL height are based on a relaxation process during which h approaches a certain equilibrium value

h_e with a time scale τ_S, i.e.:

$$\frac{dh}{dt} = \frac{(h_e - h)}{\tau_S}. \tag{6}$$

The equilibrium height h_e is often parameterised using one of the diagnostic equations given above (Eqs. (1), (2), or (3)). The time scale δ/τ_S has been proposed to be proportional, e.g., to $1/f$, to a combination of surface layer scaling variables such as L_*/u_*, or to the inverse of a normalised cooling rate $\Delta\Theta(\partial\Theta_0/\partial t)^{-1}$ where $\Delta\Theta$ is $T_h - T_0$ (subscripts h and 0 refer to $z = h$ and surface values, respectively).

The evolution of the SBL is highly non-stationary; one would thus expect that prognostic equations taking into account relevant mechanisms should be superior to each diagnostic relationship for simulating the stable MH. However, comparisons of different diagnostic and prognostic relationships with observations have not corroborated this expectation. For practical use it is also helpful that diagnostic equations do not require an initial value of the MH as input.

The verification of such diagnostic or prognostic relationships has long been performed with the aid of radiosonde data (e.g., Hanna, 1969; Yu, 1978; Mahrt and Heald, 1979; Wetzel, 1982). Since the early 1980s, sodar observations have increasingly been used for this purpose (e.g., Arya, 1981; Nieuwstadt, 1984; Koracin and Berkowicz, 1988; Beyrich, 1993, 1994b). The prognostic equations have rarely been tested at all and only single case studies are reported in the literature. For the diagnostic equations, correlation coefficients typically range between 0.4 and 0.7, quite often with large scatter. Also, the numerical constants appearing in all the parameterisations vary significantly, and it seems difficult to recommend any universal and site-independent value. Hence, there is still a need for verification studies of the different SBL height parameterisations using comprehensive data sets.

3.2.2. Modelling and parameterisation of the MH under convective conditions

Diagnostic relations based on similarity theory have a few times been suggested to parameterise the CBL depth (e.g., Tennekes, 1970; Zilitinkevich, 1972; San José and Casanova, 1988). However, these are valid only under certain conditions (e.g., free convection) and are not of much practical relevance. The *Ri*-method has been used by Vogelezang and Holtslag (1996) also for unstable situations by adding an excess temperature to the near-surface temperature, as suggested by Troen and Mahrt (1986) and described in Section 4.1.

Today, the numerical integration of mixed-layer slab models is a well-established way to simulate the evolution of the convective MH. These models

use surface fluxes and an initial temperature profile as basic input parameters. The latter one represents a general problem for these models since normally the network of radiosounding stations is not dense enough for boundary layer studies.

Prognostic equations describing the growth of the CBL are normally derived from a parameterisation of the TKE budget equation which is either averaged over the whole mixed layer or specified at the mixed layer top. The equations proposed by various authors mainly differ in the terms which are neglected in the TKE budget and how, the remaining terms are parameterised. The spectrum ranges from simply considering surface heating as the only relevant driving force (Betts, 1973; Carson, 1973; Tennekes, 1973) to additional consideration of mechanical turbulence production due to surface friction (Driedonks, 1981, 1982b), local changes of TKE at the level $z = h$ (so-called "*spin-up*" effect, Zilitinkevich, 1975; Gryning and Batchvarova, 1990; Batchvarova and Gryning, 1991), wind shear across the entrainment layer (Stull, 1976a; Driedonks, 1981; Manins, 1982; Rayner and Watson, 1991), explicit parameterisation of TKE dissipation (Zeman and Tennekes, 1977), and finally rather complex equations taking also into account energy losses in connection with gravity waves (Stull, 1976b) or the influences of moisture and advection (Steyn, 1990). A survey of these relationships is given in Seibert et al. (1998). Comparisons of some of them with observational data can be found in Driedonks (1981, 1982b), Arya and Byun (1987), or Batchvarova and Gryning (1991, 1994). These studies as well as sensitivity experiments carried out by Beyrich (1994b) have shown that the observed variability of the MH during daytime can in general be well described if surface heating and mechanical turbulence production due to surface friction are taken into account, with the entrainment heat flux parameterised in terms of the surface heat flux.

These effects are properly parameterised in the following two equations from Driedonks (1982a) and Batchvarova and Gryning (1991), respectively:

$$\frac{\mathrm{d}h}{\mathrm{d}t} = A\,\frac{Q_0}{\Delta\Theta} + B\,\frac{u_*^3}{\beta h\,\Delta\Theta} = \frac{Aw_*^3 + Bu_*^3}{\beta h \Delta\Theta}, \tag{7}$$

$$\frac{\mathrm{d}h}{\mathrm{d}t} = (1+2A)\,\frac{Q_0}{\gamma_\Theta h} + 2B\,\frac{u_*^3}{\gamma_\Theta \beta h^2} = \frac{(1+2A)w_*^3 + 2Bu_*^3}{\gamma_\Theta \beta h^2}. \tag{8}$$

The values of the constants A and B given in the literature differ considerably, ranging between 0 and 1 for A, and 0 and >10 for B. Many authors use $A = 0.2$ as a typical value (e.g., Tennekes, 1973; Yamada and Berman, 1979; Driedonks, 1982b). However, recent comparisons with measurements from different climatic regions suggest a higher typical value of $A \approx 0.4$ (e.g., Tennekes and van Ulden, 1974; Clarke, 1990; Betts, 1992; Culf, 1992). The

constant A represents the ratio $-Q_h/Q_0$ between the entrainment-layer and surface-layer heat fluxes, therefore, Carson (1973) suggested the use of different values for A corresponding to different stages of the CBL evolution. Betts and Barr (1997) found that A increases with the wind speed, but they did not include a u_*-term. For B, Tennekes (1973) proposed $B = 2.5$, a value used later also by Gryning and Batchvarova (1990). Driedonks (1981, 1982b) achieved the best agreement with observations using $B = 5$, a value also applied by, e.g., Zilitinkevich et al. (1992). The possible ranges for A and B reported in the literature significantly affect the simulated CBL growth. Beyrich (1994b) showed that a variation of their values over the typical range reported in the literature results in differences of the simulated evolution of the MH much larger than those which would originate from an application of a more complex equation. Beyrich (1995) therefore suggested to adapt the model constants to actual observations (e.g., from sodar or wind profiler data) to improve the model output results.

3.2.3. Determination of the MH from NWP model output

Dispersion models for the regional scale or for long-range transport often derive the MH from NWP model output. This may also be considered for the local scale if suitable measurements are not available at the site under consideration. It is obvious that methods and their reliability depend on the degree of sophistication of the ABL parameterisation and on the resolution of the boundary layer within the NWP model. The bulk Richardson-number method is the standard approach to derive MHs from the NWP models.

A procedure to determine h from the output of HIRLAM, the limited area model used in the Nordic and some other European countries, has been validated by Sørensen et al. (1996). It is based on a bulk Richardson number derived from the model level data:

$$Ri_b(h) = \frac{gh}{\Theta_{v1}} \frac{\Theta_v(h) - \Theta_{v1}}{U(h)^2 + V(h)^2} \tag{9}$$

where Θ_{v1} is now the virtual potential temperature at the lowest model level (about 30 m above ground). This formula is consecutively applied for $h = z_2, z_3, \ldots$, where the z_i are the model levels. The actual value of h is chosen as the height where Ri_b reaches a critical value. An optimal value of 0.25 was found after applying the method to radiosoundings with a clear convective lid. This method is used in the "Danish Emergency Response Model of the Atmosphere" (Sørensen, 1998; Sørensen et al., 1998).

Maryon and Best (1992) studied the boundary layer height h determined from vertical profiles obtained from NWPs for use in NAME (UK Met. Office's long range transport model for nuclear accidents). They compared model

boundary layer heights diagnosed by different methods with radiosonde measurements. These methods, based on identifying the level at which a critical gradient Ri-number equal to 1.3 is reached, gave generally poor results, underestimating h particularly for the daytime boundary layer. A best-fit procedure yielded a value $Ri_c = 7.2$, but the improvement was limited. Also Wotawa et al. (1996) and Fay et al. (1997) used Richardson number methods to derive MHs from NWP model output.

The EMEP MSC-W model introduced another method to derive MHs from HIRLAM output (Jakobsen et al., 1995). The mechanical MH is defined as the lowest level where the turbulent diffusion coefficient K_M is less than 1 $m^2 s^{-1}$, with K_M determined by the method of Blackadar (1979) from the Richardson number. The convective MH is the height of the adiabatic layer, after the sensible heat input of one hour has been distributed via dry-adiabatic adjustment. The MH is taken as the larger one of the two values.

4. Intercomparison of mixing height determination methods

Data sets suitable for the testing of MH routines should, according to our opinion, fulfil at least the following requirements:

(i) high frequency of radiosonde data (at least 4 ascents a day);
(ii) continuous profile information from a remote sensing instrument (sodar, lidar, wind profiler) as a second (independent), continuous data source for MH determination from measurements;
(iii) measurements of turbulent fluxes at the surface;
(iv) sufficiently uniform terrain without too much orographic influence.

It turned out that the number of such data sets is rather limited. We finally selected three data sets: SADE-campaign (Germany), Cabauw (The Netherlands) and Payerne (Switzerland); details are given in Appendix A. Only data sets of less than a full year were available. Some of the data sets continue to grow, and a new data set is being built up at Lindenberg, a meteorological observatory and aerological station of the German Weather Service. Future work should be based on these more extensive data sets.

4.1. Assessment of the parcel methods

We have tested two different versions of the parcel methods (Fig. 1). The simple parcel method (Holzworth, 1964) uses the measured virtual potential temperature Θ_v of a radiosounding at ground level, and the MH is taken as the equilibrium level of an air parcel with this temperature. In the advanced parcel method, the temperature of the parcel is given as the temperature near the

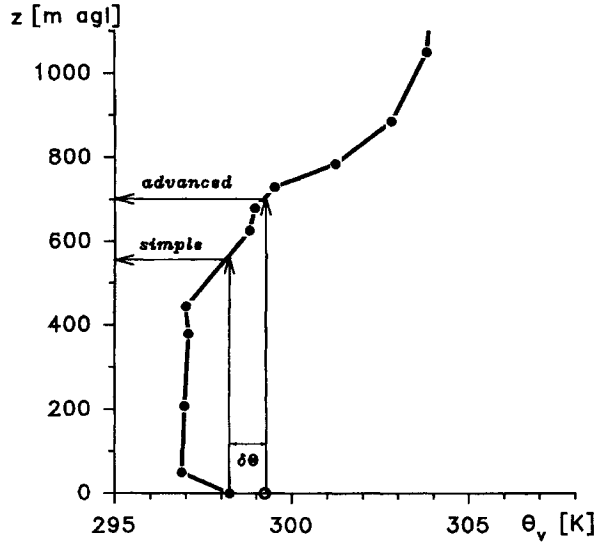

Figure 1. Illustration of the two parcel methods for the derivation of the MH in the CBL from radiosoundings. The simple parcel method uses the virtual potential temperature at ground level, while according to the advanced method an excess temperature (see Eq. (10)) is added.

ground plus an excess temperature $\delta\Theta_v$ calculated as (Troen and Mahrt, 1986; Holtslag et al., 1990; Beljaars and Betts, 1992)

$$\delta\Theta_v = \frac{C_1\langle w'\Theta_v'\rangle}{\sqrt[3]{u_*^3 + C_2 w_*^3}}. \tag{10}$$

Values of 5 and 8.5 have been suggested for C_1, while for C_2 the value of 0.6 has been used.

Since under convective conditions a superadiabatic layer is usually found near the ground, also the simple parcel method implicitly applies an excess temperature. One may thus question whether it is justified to add another excess temperature, especially as the authors who used this concept mainly applied it to NWP model output. Therefore, we plotted both the temperature excess according to Eq. (10) and the one found in radiosoundings against the heat flux (which is the dominant term in $\delta\Theta_v$) for the Cabauw data (Fig. 2). The temperature excess in the radiosounding was defined as the difference between Θ_v at the lowest level and at the first level above which the stratification was neutral or stable. Two features are striking in Fig. 2, the much higher scatter of the observed $\delta\Theta_v$ as compared to the computed one, and its larger magnitude. This implies, first, that the simple parcel method depends on stochastic influences, since its implicit $\delta\Theta_v$ is not closely related to the heat

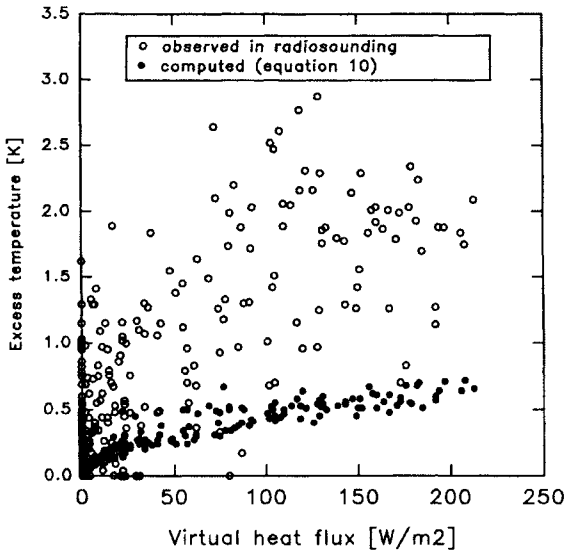

Figure 2. Excess temperatures derived from radiosoundings and computed from Eq. (10) plotted against the virtual heat flux. Radiosonde data are from De Bilt and heat flux data from Cabauw.

flux. Secondly, adding $\delta\Theta_v$ according to the similarity formula does not make much sense, as one would add only a small quantity (typically 0.5 K) to a much larger (typically 2 K) but stochastically influenced quantity. Thus, we suggest that when the advanced parcel method is applied to radiosoundings, one should omit the superadiabatic near-surface layer and instead use a larger value of the constant C_1. In order to achieve the same order of magnitude as found in the observed $\delta\Theta_v$, $C_1 = 20$ was used in this study.

This reasoning applies, to some extent, also to model data, as normal K-type diffusion parameterisation requires superadiabatic gradients to produce an upward heat flux and thus, in general, model data will already contain a certain excess temperature. This may be the reason why such a small value of the constant C_1 has been used. However, one may wonder if this mix of two excess temperatures, one created by the model and another one from similarity theory, is really adequate.

4.2. Intercomparison of empirical methods

4.2.1. Stable situations

The sodar-derived MHs during stable situations were compared with different analyses of radiosoundings for all days of the SADE intensive observa-

tion periods. The radiosoundings were subjectively analysed with respect to the temperature profile, and with Ri-number methods (with $Ri_c = 0.2$). The relationships between MHs derived from sodar and with the Ri-methods are characterised by a lot of scatter, whereas MHs from the sodar and from the temperature profile agree much better. This demonstrates that during stable situations sodar-derived MHs are strongly influenced by the shape of the temperature profile which, however, reflects the effects of mechanical turbulence production in stable situations with moderate to strong winds. The Ri-method based on the ground-level temperature yields many cases of very shallow MHs (< 50 m) whereas the sodar gives values between 50 and 200 m. It is hard to check the validity of the value of Ri_c for these circumstances of extremely shallow MHs, because if they are real, they were overestimated by the sodar which had its lowest range gate at 50 m. On the other hand, there is some uncertainty in the Ri-number method as well: if the temperature at the 20 m level is used instead of the ground-level temperature in the Ri-number (similarly to the VH-method), many Ri-number-derived MH values exceed the sodar-derived ones. This would mean that the VH-method tends to overpredict the stable MH.

Another comparison was made with the Cabauw data set, where we compared MHs under stable conditions derived from the sodar and from Ri-number analyses (Fig. 3). In contrast to SADE, the sodar MHs were derived here with a completely automatic algorithm. Like in the SADE data, Ri-number derived MHs tend to be lower than those indicated by the sodar. The number of extremely shallow MHs is much lower with the VH-method than with the standard Ri-number method. In some cases the Ri-number meth-

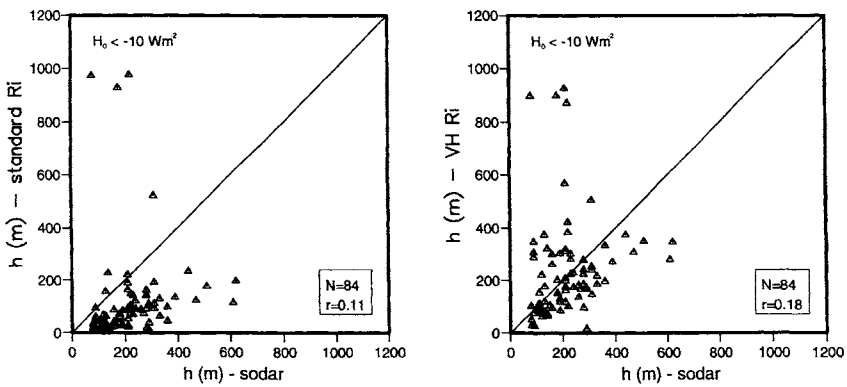

Figure 3. Scatter plots of mixing heights derived from different Ri-number methods: (Left: standard method, right: VH-method) versus sodar-derived MHs in Cabauw: for all stable hours ($H_0 < -10\ \mathrm{W\,m^{-2}}$).

ods indicate MHs around 1000 m while according to the sodar it should be below 300 m; these cases belong to the evening transition period, when the Ri-methods can pick up the height of the residual layer. Overall, the agreement between sodar-derived MHs and those obtained with the VH-method is moderate, though the sodar data tend to be somewhat higher. The correlation between MHs obtained with the standard Ri-number and from the sodar does not differ much from the correlation obtained for the VH-method, but the standard Ri-number method leads to systematically lower MHs.

During stable situations, sodars give a reasonable magnitude of the MH as long as it is not lower than the lowest sodar range gate. Sometimes they may overestimate it.

It appears difficult to judge the relative performance of the standard and the VH Ri-number method. As the critical Ri-number in the VH-method has been determined from Cabauw sodar data (obtained with an automatic routine), evaluations with other, independent data sets are necessary before final conclusions can be drawn.

4.2.2. Unstable situations

Sodars usually capture the rise of the CBL very well during a period in the morning of well-developed convective days, as long as the MH is within the sodar range. However, for a large part of the convective hours the MH is higher and it cannot be covered by sodar. There are automatic routines for MH determination by sodars, but they have the problem to recognise situations when the MH is outside the sodar range and the routine's estimates will be invalid. One automatic routine, part of a commercial sodar software (which is said to use also vertical velocities) turned out to show a lot of unexplainable variability during all times of the day in our comparison at Payerne. Unfavourable results were also found by Keder (1999).

The comparison of different methods using daytime SADE-data indicates a very good agreement between the results of the parcel method with sodar-derived MHs as well as with MHs evaluated subjectively from radiosoundings, except for a small number of outliers (Fig. 4). The agreement between the parcel method and the Ri-number method is also very good. The comparison between the standard and the advanced parcel method shows a rather small scatter while the MHs obtained with the standard parcel method are slightly lower than those from the advanced method. From the other comparisons, it appears that the advanced method is unbiased.

The advanced Ri-method (or VH method) adapted by Vogelezang and Holtslag (1996) has been used also for unstable situations with an excess temperature added to the near-surface temperature (with $C_1 = 8.5$). For the Cabauw data set, all the methods (simple parcel, advanced parcel, standard Ri-number,

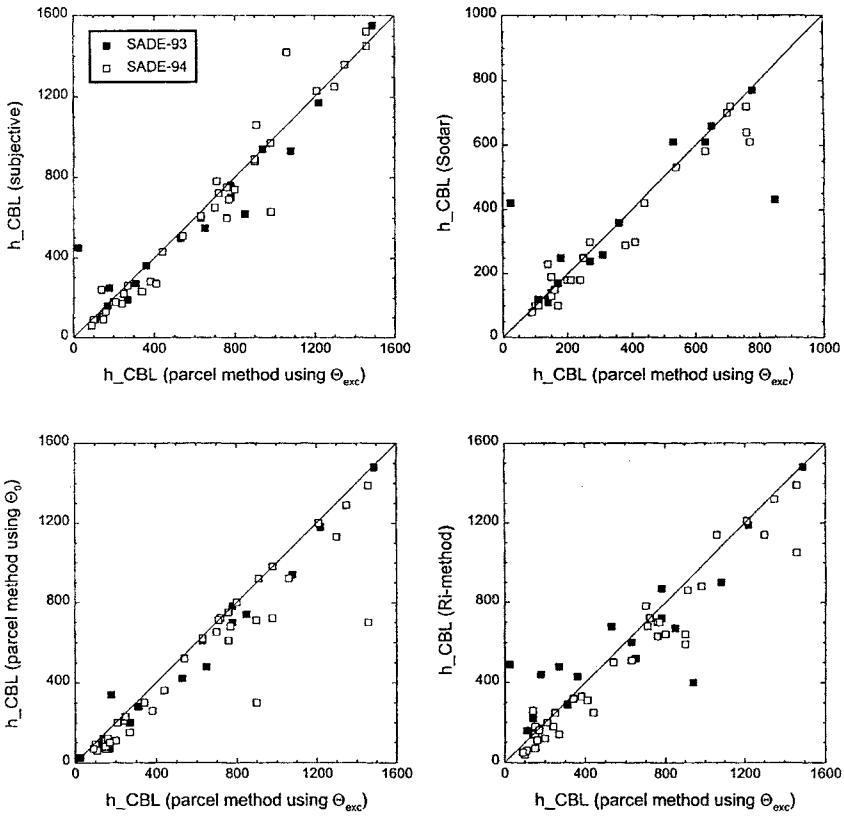

Figure 4. Scatter plot comparing a subjective evaluation of the MH based on radiosoundings (temperature, humidity, wind), a semi-objective evaluation of sodar backscatter data, the simple parcel method and the standard Ri-number method with the advanced parcel method. Data sets from SADE-93 (full symbols) and SADE-94 (open symbols), unstable hours only.

VH Ri-number) correlated well with each other ($r > 0.9$), and without significant biases (Fig. 5). The standard Ri-number method and the simple parcel methods yield almost equal results since under convective conditions, when the wind shear is usually small, Ri-number and parcel methods are almost equivalent. The comparison between the standard and the VH Ri-number method shows that the VH-method overpredicts low MHs (< 500 m, according to the standard method) as compared to the standard method, and has a weak tendency to underpredict for high MHs.

In the CBL, the Ri-number methods give very similar results to the parcel methods when the same near-ground temperature is used. Thus, we can recommend to use either the advanced parcel method or a Ri-number method

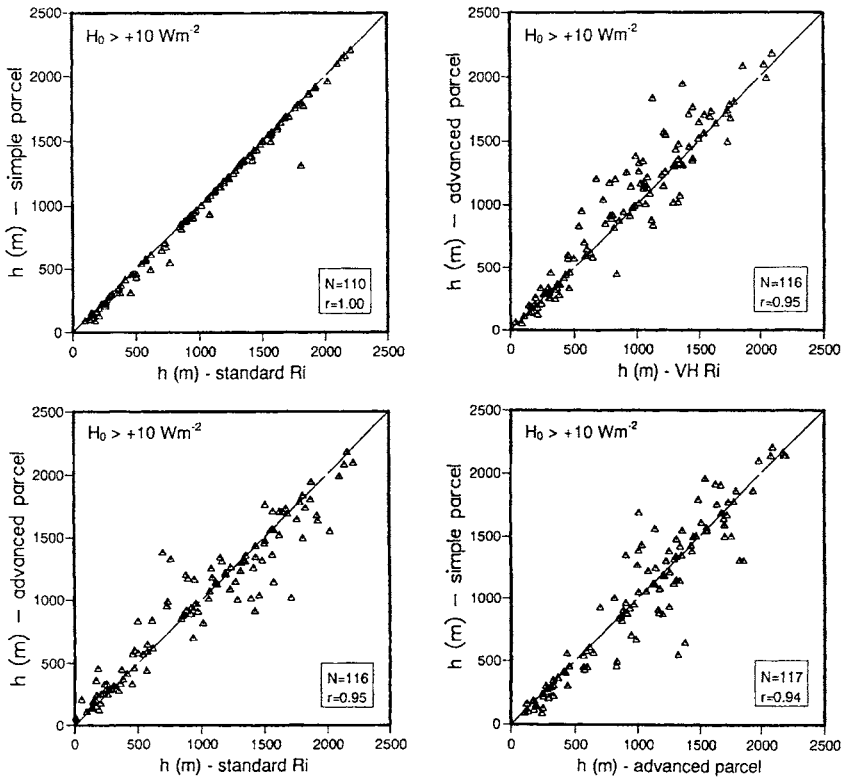

Figure 5. Scatter plot of mixing heights derived by the standard and the VH Ri-number methods as well as the simple and advanced parcel methods at Cabauw, unstable cases.

where the near-ground temperature contains an excess temperature as in the advanced parcel method (Vogelezang and Holtslag, 1996). For boundary layers where shear-produced turbulence is important, Ri-number methods should be preferred to the parcel method even if the ABL is unstable.

4.3. Intercomparison of preprocessor modules

Advanced meteorological preprocessors utilise information from both ground meteorological measurements and sounding profiles. Within the COST Action 710 we have compared five numerical preprocessors that were available to us. These were the OML meteorological preprocessor (Olesen et al., 1987), the Hybrid Plume Dispersion Model (HPDM, Hanna and Chang, 1992), the meteorological preprocessor library of Servizi Territorio (Servizi Territorio,

1994), the routine of the Finnish Meteorological Institute (Karppinen et al., 1997, 1998), and the RODOS preprocessor (Mikkelsen et al., 1997). These preprocessors are shortly described in Appendix B.

We have compared the results from the MH-modules included in these five preprocessors with each other and with the results of empirical methods for typical days of the selected data sets described in Appendix A. The empirical methods are based on radiosoundings and sodar measurements. The radiosoundings were analysed with the Ri-number method and – for hours with positive heat flux – the parcel method. Sodar-derived MHs are the only empirical method available which gave continuous information, but they are limited to night-time and shallow unstable boundary layers.

Through these intercomparisons, a number of specific problems for each preprocessor could be identified, but the cause of these problems was not always apparent. Thus, it will be a major task for the model developers to investigate them more in depth.

4.3.1. 28–29 May 1996, Payerne (Fig. 6)

OML and HPDM gave similar results during the night. However, during the convective period of the first day, OML used all the time the MH given by

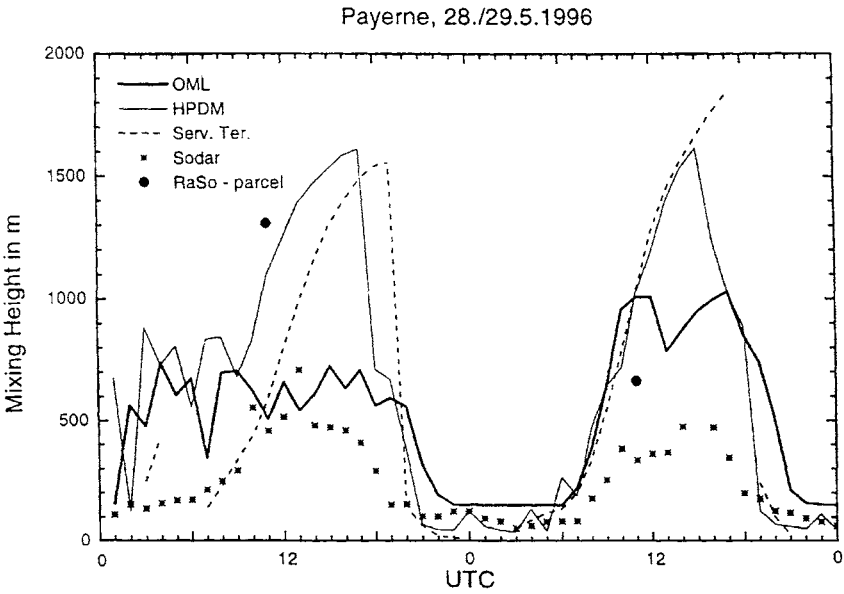

Figure 6. Evolution of the MH in Payerne, 28–29 May 1996, as computed by different preprocessors (lines) and as derived with empirical methods (symbols).

u_*/f, while HPDM produced a convective growth of the mixing layer during the day. Note the difference between the convective MHs produced by HPDM and ST on the first day, which was probably due to different initialisations. On the second day, HPDM and ST agreed well as they both start from low initial values. OML again used u_*/f, indicating that the convective MH calculated in OML was lower than the one obtained by u_*/f. During the second night, OML gave its minimum height of 150 m while other methods indicated lower MHs. During daytime, the sodar-based MHs were erroneously placed within the CBL (see discussion of sodar routines in Section 4.2).

4.3.2. 6–7 July 1995, Cabauw (Fig. 7)

On these days, OML produced a growing mixing layer during the daytime, at first determined by u_*/f (growing u_*) and then by the convective model. Compared with the sodar, the early phase of this growth was overestimated by OML (because it used the u_*/f formula which is not appropriate for this situation) while it was correct in the ST and FMI models. Later on the day, OML gave MHs which coincided with the radiosounding while the ST and RODOS model values remained lower. We cannot explain the behaviour of

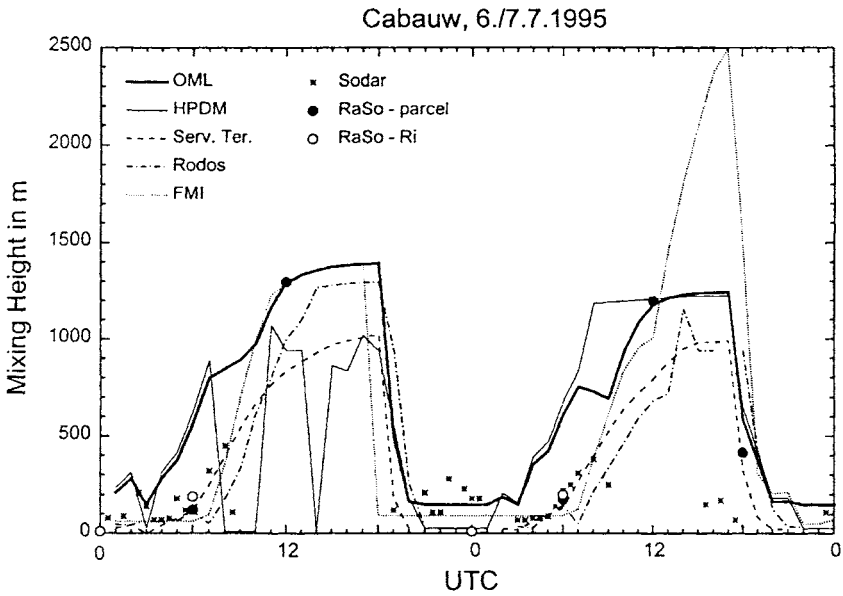

Figure 7. Evolution of the MH in Cabauw, 6–7 July 1995, as computed by different preprocessors (lines) and as derived with empirical methods (symbols).

HPDM on the first day. The plateau of the MH given by HPDM on the second day is not shown by other models. During the second day, the FMI model produced an unexplained, unrealistic growth in the afternoon. We consider the sodar values of the night from July 6 to 7 too high, but they show nicely the growth of the mixing layer on the morning of the second day, coinciding with the ST convective slab model and the morning radiosounding. However, while OML reached the correct MH at noon, ST and RODOS MHs again remained too low.

4.3.3. 12–13 November 1995, Cabauw (Fig. 8)

The sodar was able to detect the MH throughout this period, obviously connected with a strong inversion, and also picked up by the parcel method. OML detected this inversion as a "sustained lid" and just interpolated the height of this lid linearly between the radiosoundings. There was a positive heat flux only for a few hours on each of the two days, as indicated in ST-slab model. In contrast to OML, strong winds with associated high u_* caused the HPDM to yield much too high MHs in the first 30 h. The other models fluctuated around the values observed with the sodar during the whole period. With the excep-

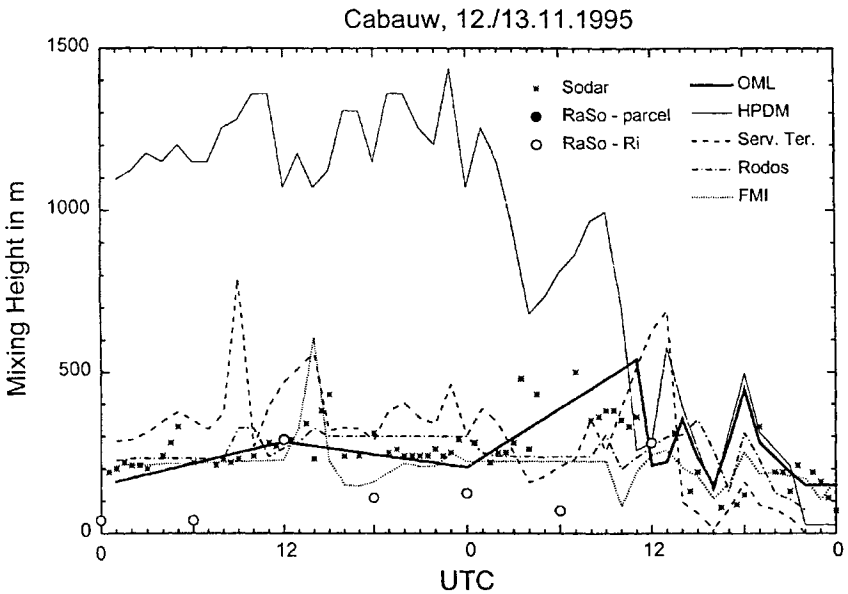

Figure 8. Evolution of the MH in Cabauw, 12–13 November 1995, as computed by different preprocessors (lines) and as derived with empirical methods (symbols).

tion of 12 UTC on the second day, the standard Ri-number method always yielded MHs considerably lower than obtained by all other methods while the VH method (not shown) gave more consistent values.

4.3.4. 7–8 October 1994, Melpitz/SADE (Fig. 9)

The OML and HPDM models showed an explosive growth of the mixing layer in the morning of the first day, while FMI, ST and RODOS started the mixing layer growth later and at a slower pace. Sodar and radiosonde data showed that HPDM and OML were not realistic. Their behaviour cannot be explained by u_* either, in contrast to some other cases. The behaviour of HPDM was even more unexpected than that of OML, which at least showed a normal convective growth phase between 1100 and 1500 m. The slab model of ST did not reach a sufficient height, due to its constant temperature gradient, while all the other models reached the correct maximum MH as indicated by the radiosoundings. On the morning of the second day, OML, FMI, RODOS and ST all created a very similar growth of the CBL which is also supported by the sodar data. However, in HPDM the MH rose until its maximum values of 3000 m. During the night between the first and the second day, all the methods and the sodar

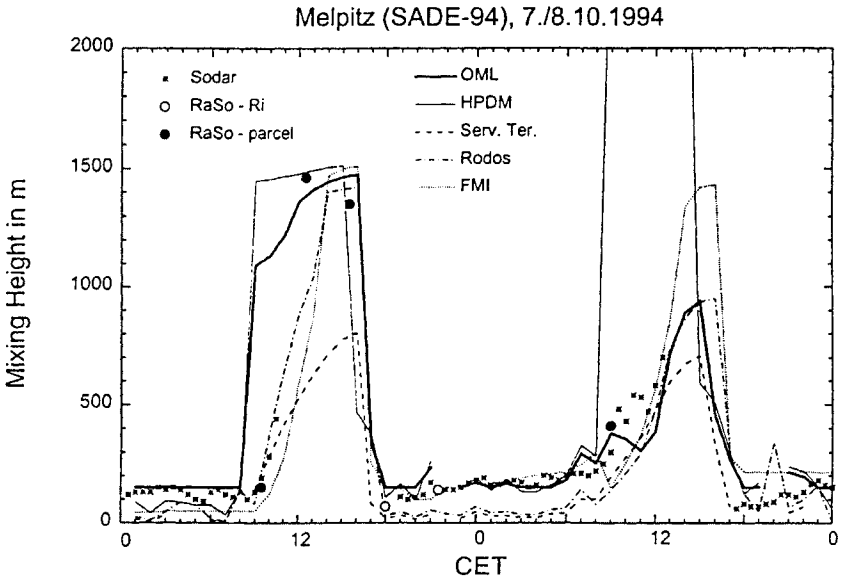

Figure 9. Evolution of the MH in Melpitz, 7–8 October 1994, as computed by different pre-processors (lines) and as derived with empirical methods (symbols).

measurements are in the same range, with exception of the ST and RODOS models which lead to considerably smaller values.

5. Conclusions and recommendations

There are two general possibilities for operational MH determination, namely the analysis of profile measurements on one hand and the application of parameterisations or models based on operationally available data on the other hand. If suitable data are available, the first option is to be preferred. Since none of the methods and models are perfect, it is recommended to have results obtained in an operational context checked by a qualified scientist, considering the basic data. It is possible to substitute NWP model output for measurements, but then the results strongly depend on the characteristics of the model, especially its ABL formulation and vertical resolution. Therefore, no general recommendations can be made here. High-resolution mesoscale models with good ABL formulation can be useful especially in complex terrain.

A flow chart for the practical determination of the MH according to available data is shown in Fig. 10. It is to be seen as a guidance but not as an algorithm which must be followed strictly. Considering the contradictions and difficulties we found, and the limited amount of data that could be used in this study, the present conclusions cannot be seen as definite ones.

5.1. Analysis of measurements

Parcel methods based on the virtual potential temperature are the most reliable ones for the detection of the convective MH. The simple parcel method already gives reasonable results. When using an excess temperature, attention has to be paid to the value to which it is added. If this is the temperature of the well-mixed CBL, a value of the constant C_1 around 20 appears to be more appropriate than the values 5 or 8.5 which have been suggested so far (see also 5.3). Methods using a bulk Richardson number can also be applied to convective boundary layers, but then they should use an excess temperature similar to the parcel methods to compute the temperature differences.

The determination of the MH in situations where mechanically produced turbulence is important is much more difficult. Given the fact that temperature and wind profiles are the most widespread information, we consider bulk Richardson number methods to be the most appropriate ones under such conditions. However, with shallow stable MHs, such methods give questionable results if the wind profile is available from radiosondes only, as such wind data may be inaccurate and/or not sufficiently well resolved near the ground. Forming a composite with wind information from other measurement systems (sodar, mast) might help to overcome this problem.

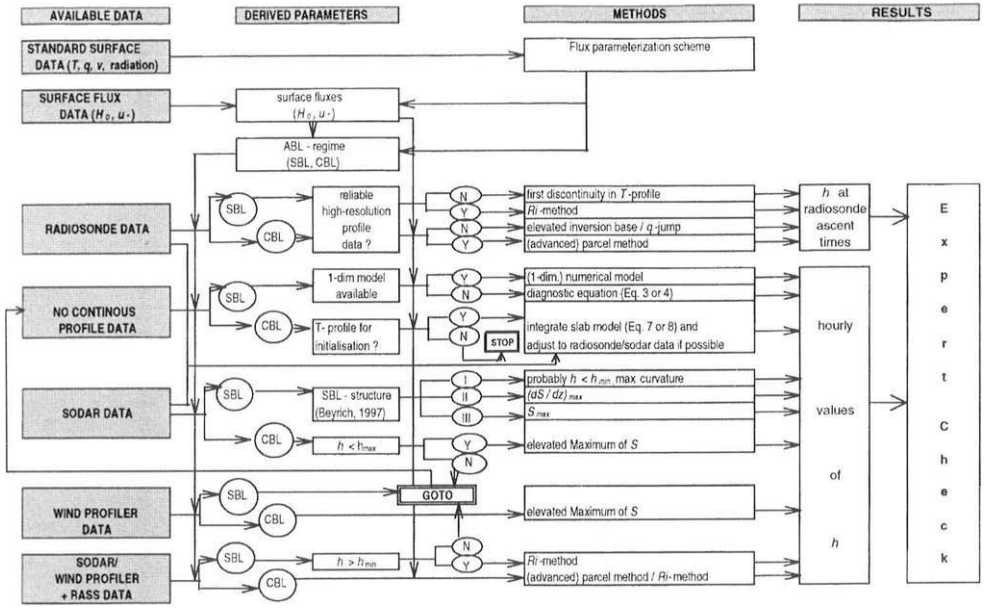

Figure 10. Flowchart to guide the practical determination of the mixing height h. The left column provides possible entries, depending on the available data. All paths which lead into the GOTO box continue to the "NO CONTINUES PROFILE DATA" entry box. STOP means that mixing height determination is not possible. S denotes the intensity of the backscattered signal of a sodar or wind profiler.

Profiles obtained with tethersondes need to be smoothed, and trends to be removed, as substantial local temperature changes may occur during the ascent or descent.

Direct determination of the MH from sodar data is possible only if the MH is well within the range of the sodar (typically, about 50 to 500 m). If it is not known whether the MH really falls into the range of the sodar, erroneous conclusions are easily possible. MH detection routines currently implemented on commercial sodars by manufacturers should be considered cautiously. End-users should have the performance of any routine carefully checked on their site, using other reliable methods for comparison.

The backscatter intensity profiles obtained from electromagnetic wind profilers (operation frequency around 1 GHz) are a promising basis for MH determination in well-developed cloudless CBLs. However, algorithms developed so far appear not to be reliable enough for operational use. In the near future, radio-acoustic sounding systems (RASS) providing temperature profiles in combination with electromagnetic or acoustic wind profilers will allow the application of Ri number methods on a continous base.

5.2. Application and improvement of preprocessors

For convective boundary layers, the numerical slab model is appropriate. Its integration should use the actual initial temperature profile, and not a predetermined value of the gradient of Θ_v above the mixing layer. Rate equations in such models should include also the mechanical contribution to mixing layer growth, parameterised by u_*.

For the mechanically-driven MH, all the current preprocessors rely on similarity formulae involving u_*, f, and partly also L_*; when using such formulae, Eq. (3) (Nieuwstadt, 1981) is to be preferred to the simple u_*/f approach for stable conditions. However, we regard this approach as not satisfactory from a physical point of view (see Section 3.2), and it is not applicable in low latitudes. Richardson-number methods appear to be better in this respect (input data may be a problem, however). Using numerical models may become a solution in the future.

Preprocessors should allow the substitution of measured data for parameterised ones at any stage, even if they do not follow idealised parameterisations: e.g., if there are periods of downward heat flux during the day or upward heat flux during the night.

Preprocessors should be able to use all soundings available, not just those at the standard hours 00 and 12 UTC. The real launching time of the sounding should be considered, as it may vary by about one hour around the standard time.

Preprocessors should be able to work with high-resolution radiosonde data (e.g., readings every 2 to 10 s) and not only with significant levels as reported in the TEMP part B. This requires appropriate dimensioning of the arrays in the code as well as taking into account the presence of small fluctuations in the high-resolution data, which may, e.g., lead to relatively strong potential temperature gradients over small layers in a well-mixed CBL. The preferred solution would be, in addition to the archival of full resolution data, to provide TEMP part B data with enhanced resolution in the lower atmospheric layers.

Constants and parameters specific to a certain climatic region (e.g., absolute maxima or minima of the MH, or criteria to find convective lids) should be clearly documented, and users should have the possibility to change them.

5.3. Future research

The suitability of the parcel method for the analysis of temperature profiles in the CBL calls for studies on both the practical determination of the mean temperature from an arbitrary sounding (including cases where the ABL is not really well-mixed) and the determination of the constants in the calculation of the excess temperature.

There is a general need for more work on the SBL. Formulae for the mechanical MH, especially those based on Richardson numbers, should be tested on more data sets. The effects of intermittent turbulence and of waves in the outer SBL on the dispersion of pollutants should be studied, too.

The development of routines to derive the MH in deep CBLs from the backscatter intensity profile of electromagnetic wind profilers should be continued with the aim of operational applicability. Such work would ideally include sodar data to detect MHs below the lowest profiler range gates, especially under stable conditions. Supplementing this chain of profilers with minisodars for very shallow MHs should be considered.

The spatial and temporal representativity of MHs derived from measurements (including indirect effects, such as, e.g., those of the initial profile and the heat flux in CBL slab models) should be studied. Parameterisations of the entrainment zone (Gryning and Batchvarova, 1994; Beyrich and Gryning, 1998) and the influence of waves, wind shear and synoptic-scale vertical motion at the CBL top on the MH development should be further investigated.

Numerical simulation models using a prognostic equation for the turbulent kinetic energy (closure of the order 1.5 or higher) should be considered as an alternative to simple parameterisations in the future. Where spatial inhomogeneities are relevant, three-dimensional models must be used. As long as computer resources do not allow their application for long data series, one-dimensional models could be considered in simple terrain.

If NWP models are to provide input for dispersion modelling, specific data requirements, different from those of weather forecasting, should be taken into account. For example, better temporal resolution of the NWP model output or providing additional variables such as TKE, diffusion coefficients or parameters describing deep convection (venting of the ABL) would be desirable.

It should be investigated whether subsidence velocities and horizontal advection at the top of the CBL obtained from NWP model output (presently the only practical source) are reliable enough to improve the performance of CBL models. Techniques to fit parameterisations and models to observed data, such as variational methods, should be developed and implemented. We believe that this is the most important improvement which can be made to CBL slab models.

Last but not least, we recommend to establish long-term monitoring programmes for the ABL in different climatic regions, including measurements of the surface energy budget components, turbulence parameters at several levels, at least two continuous profiling systems, and radiosoundings. This goal could be accomplished by supplementing existing field sites. Further development of remote sounding systems in order to measure turbulence parameters accurately would bring considerable benefits for MH determination.

Acknowledgements

The authors of this report acknowledge the support given by COST through the European Commission and (P. Tercier) the Swiss Government. Data for the comparisons have kindly been supplied by the KNMI, the Institute of Meteorology and Climate Research at the Research Centre of Karlsruhe, the Meteorological Institute of the University of Munich, and the Institute of Troposphere Research in Leipzig. Ari Karppinen from the Finnish Meteorological Institute ran the FMI model for the computations of Section 4.3.

Appendix A. Data sets used for testing mixing height routines

A.1. Cabauw (1995/96)

Cabauw is a boundary layer study site operated by the Royal Netherlands Meteorological Institute KNMI (Monna and van der Vliet, 1987). It is located between Utrecht and Rotterdam (51°58′N, 4°56′E, 2 m), surrounded mainly by pastures and meadows with interspersed small water channels. Turbulent fluxes of sensible and latent heat are available, derived by different methods. A sodar without Doppler capabilities is operated on the site; it is used to derive

MH from the backscatter profile. The data used in this study cover the period from July 1995 until January 1996. In addition to the on-site data, regular aerological soundings from the station De Bilt, which is about 25 km north-east of Cabauw, have been used.

A.2. Payerne 1995/96

Payerne is the aerological station of the Swiss Meteorological Institute located in the western part of the Swiss Midland (46°49′N, 6°57′E, 491 m). The Swiss Midland is a hilly basin surrounded to the north by the Jura mountains and to the south by the Alps. The data relevant for this study comprise routine aerological soundings, measurements of the sensible heat and the momentum flux, and data obtained from a Remtech PA1 Doppler sodar and a Radian LAP-3000 1290 MHz wind profiler. Several periods between August 1995 and June 1996 have been chosen for the investigation.

A.3. SADE (1993/94)

The SADE-93 and SADE-94 experiments were carried out at the field site Melpitz (51°32′N, 12°54′E, 87 m) about 40 km NE of the city of Leipzig. Melpitz is a flat-terrain site situated within relatively large agricultural fields and pastures. The analysis within this study focussed on three intensive observation periods: 18–23 September 1993, 20–30 September 1994, and 6–11 October 1994. For the MH determination, data from the Doppler-sodar ECHO-1D and from frequent radiosoundings were used. Surface fluxes were derived from gradient measurements and from eddy-correlation measurements.

Appendix B. Computer routines to derive mixing height values

B.1. The OML meteorological preprocessor (Olesen et al., 1987)

The meteorological preprocessor of the Danish dispersion model OML contains a module for the MH calculation. Each hour, the module computes a mechanical and, during daytime, a convective MH and selects the larger one as the actual value, but a minimum value of 150 m is applied. The mechanical MH is calculated as $h = 0.25u_*/f$ (Eq. (1)). The convective MH is obtained from the integration of the (prognostic) Eq. (7) with $A = 0.2$ and $B = 5$. It starts with the observed temperature profile, and uses observed or parameterised hourly values of u_* and Q_0. If a so-called convective lid is found in the noon sounding, the calculated convective MHs before noon are multiplied by the ratio of the base height of this lid to the calculated MH for 11 UTC. If a so-called sustained lid is found also in the following midnight sounding, the interpolated lid height is used as an upper bound for the MH.

B.2. The HPDM meteorological preprocessor (Hanna and Chang, 1992)

The meteorological preprocessor of the Hybrid Plume Dispersion Model (HPDM) produces time series of hourly values of the surface heat and momentum fluxes and of the mixing depth, using observations of wind speed, cloudiness, surface roughness length, surface moisture availability and albedo. Since the preprocessor in its standard form does not accept observed fluxes, the source code was modified in the present study in order to use measured fluxes. HPDM uses Eq. (3) (Nieuwstadt, 1981) to estimate the MH at night. During daytime, two separate MHs are calculated. One is obtained with Carson's (1973) prognostic formula (first term in Eq. (8)) which parameterises the entrainment heat flux as a fraction A of the surface heat flux ($A = 0.2$). A second MH is calculated, according to a suggestion of Weil and Brower (1983), considering solely the growth rate of the CBL due to mechanical turbulence. Finally, the larger value is taken as the convective MH. For neutral conditions (defined as Pasquill stability category D), Eq. (1) is used with $a_1 = 0.3$.

B.3. The meteorological preprocessor library of Servizi Territorio (1994)

The aim of Servizi Territorio was to offer a library of subroutines as a flexible tool which can be applied in different environments. One set of subroutines is provided for the computation of the ABL parameters. For convective MH (daytime), the so-called encroachment model (first term of Eq. (8) with $A = 0$) or the full mixed-layer growth model (Eq. (8)) are offered. Both routines assume a constant lapse rate above the top of the mixing layer throughout the day, to be taken from an early morning temperature sounding. For neutral and stable MH (night-time) the library includes Nieuwstadt's (1981) Eq. (3), Zilitinkevich's (1972) Eq. (2) with $a_2 = 0.4$, and Eq. (1). If $L_* < 0$, only Eq. (1) can be used. In all the formulae, f is set to $10^{-4}\ \mathrm{s}^{-1}$, but partly absorbed into the constants.

B.4. The FMI Routine (Karppinen et al., 1997, 1998)

The module used for the calculation of the MH at the Finnish Meteorological Institute considers 3 cases.

B.4.1. Wintertime situations

During Finnish winter the boundary layer is mostly stable or near neutral, even during daytime, and h can be estimated as a function of the friction velocity (Eq. (1)), with the coefficient estimated from the 00 and 12 UTC soundings.

B.4.2. Summer night situations

A summer night is a period when the ABL is stable with unstable sections at both ends of the nocturnal period. After sunset the thickness of the developing shallow inversion h_{inv} is assumed to keep increasing through the course of the night. The MH is expressed by the bulk formulae of Stull (1983a, b) using the integrals of Q_0 over time. If the height h given by Eq. (1) with $a_1 = 0.2$ is larger than that of the previous evening's unstable boundary layer prevailing at sunset, the latter value is used.

B.4.3. Summer day situations

Daytime is defined by an upward turbulent heat flux. The evolution of the CBL is simulated by solving numerically the standard slab model (Tennekes, 1973; Driedonks and Tennekes, 1984) leading to a system of equations similar to Eq. (7) but with an additional term in the denominator containing the velocity scale $w_{\mathrm{M}} = (w_*^3 + C_\tau u_*^3)^{1/3}$. After solving the equations for the whole period, the height h is compared to the 12 UTC sounding and corrected if necessary. The solution of the equations is continuously checked against the potential temperature observed at 2 m. If the sounding shows that the situation is not unstable as had been suggested by the energy budget method, u_*, Q_*, and L_* are replaced by profile estimates obtained from the lowest layer of the 12 UTC sounding data.

B.5. The RODOS preprocessor (Mikkelsen et al., 1996; Mikkelsen and Desiato, 1993)

MET-RODOS is a comprehensive atmospheric transport and diffusion module, designed for operational use within the real-time, on-line emergency management system RODOS. The MH can be calculated from NWP model output utilising the bulk Richardson number method with $Ri_{\mathrm{c}} = 0.25$, or from measurements.

During daytime, the mixed-layer growth model (Eq. (8)) is used. The integration starts with an initial value of h equal to 50 m; the lapse rate is taken from the previous midnight sounding. The MH during night is calculated with Nieuwstadt's (1981) formula (Eq. (3)). In the case of an upward heat flux at night or a downward heat flux during the day, the MH is calculated using Eq. (1) with $a_1 = 0.3$. In addition, if a strong inversion (lid) is found above 150 m, the MH is calculated using a bulk Richardson number formulation (Eq. (5)) with $Ri_{\mathrm{c}} = 3.0$. If this lid is lower than the MH calculated otherwise, it is taken as the MH. The lid height is not interpolated in time.

References

Andrén, A., 1995. The structure of the stably stratified atmospheric boundary layer: a large-eddy simulation study. Quarterly Journal of the Royal Meteorological Society 121, 961–986.

Anfossi, D., Bacci, P., Longhetto, A., 1976. Forecasting of vertical temperature profiles in the atmosphere during nocturnal radiation inversions from air temperature trend at screen height. Quarterly Journal of the Royal Meteorological Society 102, 173–180.

Angevine, W.M., White, A.B., Avery, S.K., 1994a. Boundary layer depth and entrainment zone characterisation with a boundary-layer profiler. Boundary-Layer Meteorology 68, 375–385.

Angevine, W.M., Trainer, M., Parrish, D.D., Buhr, M.P., Fehsenfeld, F.C., Kok, G.L., 1994b. Wind profiler mixing depth and entrainment measurements with chemical applications. Proceedings of Eigth AMS Conference on Air Pollution Meteorology and AWMA, Nashville, pp. 32–34.

Aron, R., 1983. Mixing height – an inconsistent indicator of potential air pollution concentrations. Atmospheric Environment 17, 2193–2197.

Arya, S.P.S., 1981. Parameterizing the height of the stable atmospheric boundary layer. Journal of Applied Meteorology 20, 1192–1202.

Arya, S.P.S., Byun, D.W., 1987. Rate equations for the planetary boundary layer depth (urban vs. rural). In: Modeling the Urban Boundary Layer. Amer. Meteorol. Soc., Boston, pp. 215–251.

Asimakopoulos, D.N., Helmis, C.G., Petrakis, M., 1996. Mini-acoustic sounding – a powerful tool for ABL applications: recent advances and applications of acoustic mini-sodars. Boundary-Layer Meteorology 81, 49–61.

Bacci, P., Giraud, C., Longhetto, A., Richiardone, R., 1984. Acoustic sounding of land and sea breezes. Boundary-Layer Meteorology 28, 187–192.

Batchvarova, E., Gryning, S.E., 1991. Applied model for the growth of the daytime mixed layer. Boundary-Layer Meteorology 56, 261–274.

Batchvarova, E., Gryning, S.-E., 1994. Applied model for the height of the daytime mixed layer and the entrainment zone. Boundary-Layer Meteorology 71, 311–323.

Batchvarova, E., Cai, X., Gryning, S.E., Steyn, D., 1999. Modelling internal boundary layer development in a region with complex coastline. Boundary-Layer Meteorology 90, 1–20.

Baxter, R.A., 1991. Determination of mixing heights from data collected during the 1985 SCCCAMP field program. Journal of Applied Meteorology 30, 598–606.

Beljaars, A.C.M., Betts, A.K., 1992. Validation of the boundary layer representation in the ECMWF model. ECMWF Seminar Proceedings: Validation of Models over Europe, Vol. II. Reading, UK, 7–11 September 1992.

Betts, A.K., 1973. Non-precipitating cumulus convection and its parameterisation. Quarterly Journal of the Royal Meteorological Society 99, 178–196.

Betts, A.K., 1992. FIFE atmospheric boundary layer budget methods. Journal of Geophysical Research 97, 18,523–18,531.

Betts, A.K., Barr, A.G., 1997. First international satellite land surfcase climatology Field Experiment 1987 sonde budget revisited. Journal of Geophysical Research 101, 23,285–23,288.

Betts, A.K., Albrecht, B.A., 1987. Conserved variable analysis of the convective boundary layer thermodynamic structure over tropical oceans. Journal of the Atmospheric Sciences 44, 83–99.

Beyrich, F., 1993. On the use of sodar data to estimate mixing height. Applied Physics B 57, 27–35.

Beyrich, F., 1994a. Sodar observations of the stable boundary layer height in relation to the nocturnal low-level jet. Meteorologische Zeitschrift (N.F.) 3, 29–34.

Beyrich, F., 1994b. Bestimmung der Mischungsschichthöhe aus Sodar-Daten unter Verwendung numerischer Modellrechnungen. Frankfurt/M.: Wiss.-Verlag Dr. W. Maraun (ISBN 3-927548-67-7). Schriftenreihe des FhI für Atmosphärische Umweltforschung Garmisch-Partenkirchen, Bd. 28, 161 pp. + Appendix.

Beyrich, F., 1995. Mixing height estimation in the convective boundary layer using sodar data. Boundary-Layer Meteorology 74, 1–18.

Beyrich, F., 1997. Mixing height estimation from sodar data – a critical discussion. Atmospheric Environment 31, 3941–3954.

Beyrich, F., Görsdorf, U., 1995. Composing the diurnal cycle of mixing height from simultaneous sodar and wind profiler measurements. Boundary-Layer Meteorology 76, 387–394.

Beyrich, F., Gryning, S.-E., 1998. Estimation of the entrainment zone depth in a shallow convective boundary layer from sodar data. Journal of Applied Meteorology 37, 255–268.

Beyrich, F., Güsten, H., Sprung, D., Weisensee, U., 1996. Comparative analysis of sodar and ozone profile measurements in a complex structured boundary layer and implications for mixing height estimation. Boundary-Layer Meteorology 81, 1–9.

Beyrich, F., Klose, B., 1988. Some aspects of modeling low-level jets. Boundary-Layer Meteorology 43, 1–14.

Beyrich, F., Weill, A., 1993. Some aspects of determining the stable boundary layer depth from sodar data. Boundary-Layer Meteorology 63, 97–116.

Blackadar, A.K., 1979. High resolution models of the planetary boundary layer. In: Pfafflin, J.R., Zeigler, E.N. (Eds.), Advances in Environmental Science and Engineering, Vol. 1. Gordon and Breach, New York, pp. 50–85.

Brost, R.A., Wyngaard, J.C., 1978. A model study of the stably stratified planetary boundary layer. Journal of the Atmospheric Sciences 35, 1427–1440.

Carson, D.J., 1973. The development of a dry inversion-capped convectively unstable boundary layer. Quarterly Journal of the Royal Meteorological Society 99, 450–467.

Caughey, S.J., 1982. Observed characteristics of the atmospheric boundary layer. In: Nieuwstadt, F.T.M., van Dop, H. (Eds.), Atmospheric Turbulence and Air Pollution Modeling. Reidel Publ. Co., Dordrecht, pp. 107–158.

Clarke, R.H., 1990. Modeling mixed layer growth in the Koorin experiment. Australian Meteorological Magazine 38, 227–234.

Clifford, S.F., Kaimal, J.C., Lataitis, R.J., Strauch, R.G., 1994. Ground-based remote profiling in atmospheric studies: an overview. Proceedings of IEEE 82 (3), 313–355.

Coulter, R.L., 1979. A comparison of three methods for measuring mixing layer height. Journal of Applied Meteorology 18, 1495–1499.

Culf, A., 1992. An application of simple models to Sahelian convective boundary layer growth. Boundary-Layer Meteorology 58, 1–18.

Delage, Y., 1974. A numerical study of the nocturnal boundary layer. Quarterly Journal of the Royal Meteorological Society 100, 351–364.

Devara, P.C.S., Raj, P.E., Murthy, B.S., Pandithurai, G., Sharma, S., Vernekar, K.G., 1995. Intercomparison of nocturnal lower-atmospheric structure observed with lidar and sodar techniques at Pune, India. Journal of Applied Meteorology 34, 1375–1383.

Dohrn, R., Raschke, E., Bujnoch, A., Warmbier, G., 1982. Inversion structure heights above the city of Cologne (Germany) and a rural station nearby as measured with two sodars. Meteorologische Rundschau 35, 133–144.

Dörnbrack, A., 1989. Approximative Berechnung turbulenter Flüsse und des Tensors der turbulenten Diffusion auf der Grundlage einer Schließung 2. Ordnung. Dissertation, Humboldt-Univ. Berlin, 138 S.

Driedonks, A.G.M., 1981. Dynamics of the well-mixed atmospheric boundary layer. De Bilt: KNMI Sci. Rep. WR 81–2, 189 pp.

Driedonks, A.G.M., 1982a. Sensitivity analysis of the equations for a convective mixed layer. Boundary-Layer Meteorology 22, 475–480.

Driedonks, A.G.M., 1982b. Models and observations of the growth of the atmospheric boundary layer. Boundary-Layer Meteorology 23, 283–306.

Driedonks, A.G.M., Tennekes, H., 1984. Entrainment effects in the well-mixed atmospheric boundary layer. Boundary-Layer Meteorology 30, 75–105.

Dupont, E., 1991. Étude méthodologique et expérimentale de la couche limite atmosphérique par télédetection laser. Ph.D. Thesis, Univ. Paris VI, 220 pp.

Dye, T.S., Lindsay, C.G., Anderson, J.A., 1995. Estimates of mixing depth from boundary layer radar profilers. Proceedings of 9th AMS Symposium on Meteorological Instruments & Obs., Charlotteville, pp. 156–160.

Engelbart, D., 1998. Determination of boundary-layer parameters using windprofiler/RASS and sodar/RASS. Proceedings of 9th International Symposium on Acoustic Remote Sensing (ISARS'98), Vienna, Austria. Österr. Beiträge zu Meteorologie und Geophysik 17, 192–195.

Estournel, C., Guedalia, D., 1990. Improving the diagnostic relation for the nocturnal boundary layer height. Boundary-Layer Meteorology 53, 191–198.

Etling, D., Wippermann, F., 1975. The height of the planetary boundary layer and of the surface layer. Beitraege Phys. Atmos. 48, 250–254.

Fay, B., Schrodin, R., Jacobsen, I., Engelbart, D., 1997. Validation of mixing heights derived from the operational NWP models at the German Weather Service. In: The Determination of the Mixing Height – Current Progress and Problems. EURASAP Workshop Proceedings, 1–3 Oct 1997, Report Risø-R-997(EN), ISBN 87-550-2325-8, Risø National Laboratory, Roskilde, Denmark, pp. 55–58.

Fisher, B.E.A., Erbrink, J.J., Finardi, S., Jeannet, P., Joffre, S., Morselli, M.G., Pechinger, U., Seibert, P., Thomson D.J. (Eds.), 1998. COST Action 710-Final Report. Harmonisation of the pre-processing of meteorological data for atmospheric dispersion models. L-2985 European Commission, Luxembourg, EUR 18195 EN (ISBN 92-828-3302-X).

Fitzharris, B.B., Turner, A., McKinley, W., 1983. Cold season inversion frequencies as measured with acoustic sounder in the Cromwell Basin. New Zealand Journal of Science 26, 307–313.

Garrett, A.J., 1981. Comparison of observed mixed layer depth to model estimates using observed temperature and winds, and MOS forecasts. Journal of Applied Meteorology 20, 1277–1283.

Garratt, J.R., 1982a. Observations in the nocturnal boundary layer. Boundary-Layer Meteorology 22, 21–48.

Garratt, J.R., 1982b. Surface fluxes and the nocturnal boundary layer height. Journal of Applied Meteorology 21, 725–729.

Garratt, J.R., 1992. The Atmospheric Boundary Layer. University Press, Cambridge, 316 pp.

Gaynor, J.E., Ye Jin Ping, White, A.B., 1994. Determining mixing depths in complex terrain near a power plant with radar profiler reflectivities. Proceedings of 8th AMS Conference on Air Pollution Meteorology & AWMA, Nashville, pp. 335–339.

Gland, H., 1981. Qualifying test on a three-dimensional Doppler-sodar (Satolas: July–December 1980). Electricité de France, Paris, Report EDF HE/32-81.9, 36 pp.

Godowitch, J.M., Ching, K.S., Clarke, J.F., 1985. Evolution of the nocturnal inversion layer at an urban and nonurban location. Journal of Climate and Applied Meteorology 24, 791–804.

Görsdorf, U., Lehman, V., 2000. Enhanced accuracy of RASS measured temperatures due to an improved range correction. Journal of Atmospheric and Oceanic Technology, in print.

Gryning, S.-E., Batchvarova, E., 1990. Analytical model for the growth of the coastal internal boundary layer during onshore flow. Quarterly Journal of the Royal Meteorological Society 116, 187–203.

Gryning, S.-E., Batchvarova, E., 1994. Parametrization of the depth of the entrainment zone above the daytime mixed layer. Quarterly Journal of the Royal Meteorological Society 120, 47–58.

Hanna, S.R., 1969. The thickness of the planetary boundary layer. Atmospheric Environment 3, 519–536.

Hanna, S.R., 1992. Effects of data limitations on hopes for improved short range atmospheric dispersion models. In: Olesen, H.R., Mikkelsen, T. (Eds.), Proceedings of Workshop "Objec-

tives for next-generation of practical short-range atmospheric dispersion models" (Risø, 1992). DCAR Roskilde, pp. 77–85.

Hanna, S.R., Burkhart, C.L., Paine, R.J., 1985. Mixing height uncertainties. Proceedings of 7th AMS Symposium on Turbulence and Diffusion, Boulder, pp. 82–85.

Hanna, S.R., Chang, J.C., 1992. Boundary-layer parameterizations for applied dispersion modeling over urban areas. Boundary-Layer Meteorology 58, 229–259.

Hayashi, M., 1980. Acoustic sounding of the lower atmospheric inversion layer. Journal of the Meteorology Society of Japan 58, 194–201.

Hicks, R.B., Smith, D., Irwin, P.J., Mathews, T., 1977. Preliminary studies of atmospheric acoustic sounding at Calgary. Boundary-Layer Meteorology 12, 201–212.

Holtslag, A.A.M., De Bruin, E.I.F., Pan, H.-L., 1990. A high resolution air mass transformation model for short range weather forecasting. Monthly Weather Review 118, 1561–1575.

Holzworth, C.G., 1964. Estimates of mean maximum mixing depths in the contiguous United States. Monthly Weather Review 92, 235–242.

Holzworth, C.G., 1967. Mixing depths, wind speeds and air pollution potential for selected locations in the United States. Journal of Applied Meteorology 6, 1039–1044.

Holzworth, C.G., 1972. Mixing depths, wind speeds, and potential for urban pollution throughout the contiguous United States. EPA, Office of Air Programs Publ. AP-101, 118 pp. (Can be obtained from EPA, Research Triangle Park NC 277711, USA).

Jakobsen, H.A., Berge, E., Iversen, T., Skålin, R., 1995. Status of the development of the multilayer Eulerian model. EMEP/MSC-W Note 3/95 (can be obtained from: Norwegian Meteorological Institute, P.O. Box 43, N-0313 Oslo 3, Norway).

Joffre, S.M., 1981. The physics of the mechanically driven atmospheric boundary layer as an example of air–sea ice interaction. Univ. of Helsinki, Dept. of Meteorology Rep. No. 20, 75 pp.

Jones, D.E., 1985. Mixing depth in La Trobe Valley. Clean Air in Australia 19, 49–51.

Kaimal, J.C., Abshire, N.L., Chadwick, R.B., Decker, M.T., Hooke, W.H., Kroepfli, R.A., Neff, W.D., Pasqualucci, F., Hildebrand, P.H., 1982. Estimating the depth of the daytime convective boundary layer. Journal of Applied Meteorology 21, 1123–1129.

Karppinen, A., Kukkonen, J., Nordlund, G., Rantakrans, E., Valkama, I., 1998. A dispersion modelling system for urban air pollution. Finnish Meteorological Institute: Publications on Air Quality 28. Helsinki, 58 pp.

Karppinen, A., Joffre, S., Vaajama, P., 1997. Boundary layer parametrization for Finnish regulatory dispersion models. International Journal of Environment and Pollution 8, 557–564.

Keder, J., 1999. Detection of inversions and mixing height by REMTECH PA2 sodar in comparison with collocated radiosonde measurements. Meteorology and Atmospheric Physics 71, in print.

Kitaigorodskii, S.A., Joffre, S.M., 1988. In search of a simple scaling for the height of the stratified atmospheric boundary layer. Tellus 40A, 419–433.

Klein Baltink, H., Holtslag, A.A.M., 1997. A comparison of boundary-layer heights inferred from windprofiler backscatter profiles with diagnostic calculations using regional model forecasts. Proc. EURASAP Workshop on The Determination of the Mixing Height – Current Progress and Problems, Risø National Laboratory, Denmark, 51–54.

Klöppel, M., Stilke, G., Wamser, C., 1978. Experimental investigations into variations of ground based inversions and comparison with results of simple boundary layer models. Boundary-Layer Meteorology 15, 135–145.

Koracin, D., Berkowicz, R., 1988. Nocturnal boundary layer height: observations by acoustic sounders and prediction in terms of surface layer parameters. Boundary-Layer Meteorology 43, 65–83.

Kurzeja, R.J., Berman, S., Weber, A.H., 1991. A climatological study of the nocturnal planetary boundary layer. Boundary-Layer Meteorology 54, 105–128.

Mahrt, L., 1981. Modeling the depth of the stable boundary layer. Boundary-Layer Meteorology 21, 3–19.

Mahrt, L., Heald, R.C., 1979. Comments on determining the height of the nocturnal boundary layer. Journal of Applied Meteorology 18, 383.

Mahrt, L., Heald, R.C., Lenschow, D.H., Stankov, B.B., Troen, I., 1979. An observational study of the structure of the nocturnal boundary layer. Boundary-Layer Meteorology 17, 247–264.

Mahrt, L., André, J.C., Heald, R.C., 1982. On the depth of the nocturnal boundary layer. Journal of Applied Meteorology 21, 90–92.

Manins, P.C., 1982. The daytime planetary boundary layer: A new interpretation of Wangara data. Quarterly Journal of the Royal Meteorological Society 108, 689–705.

Marsik, F.J., Fischer, K.W., McDonald, T.D., Samson, P.J., 1995. Comparison of methods for estimating mixing height used during the 1992 Atlanta Field Initiative. Journal of Applied Meteorology 34, 1802–1814.

Martin, C.L., Fitzjarrald, D., Garstang, M., Oliveira, A.P., Greco, S., Browell, E., 1988. Structure and growth of the mixing layer over the Amazonian rain forest. Journal of Geophysical Research 93, 1361–1375.

Maryon, R.H., Best, M.J., 1992. 'NAME', 'ATMES' and the boundary layer problem. Met O (APR) Turbulence and Diffusion Note No. 204 (U.K. Met. Office).

Mason, P.J., Derbyshire, S.H., 1990. Large-eddy simulation of the stably stratified atmospheric boundary layer. Boundary-Layer Meteorology 53, 117–162.

McElroy, J.L., Smith, T.B., 1991. Lidar descriptions of mixed layer thickness characteristics in a complex terrain/coastal environment. Journal of Applied Meteorology 30, 585–597.

Mikkelsen, T., Desiato, F., 1993. Atmospheric dispersion models and pre-processing of meteorological data for real-time application. Radiation Protection Dosimetry 50, 205–218.

Mikkelsen, T., Thykier-Nielsen, S., Astrup, P., Santabarbara, J.M., Sørensen, J.H., Rasmussen, A., Robertson, L., Ullerstig, A., Deme, S., Martens, R., Bartzis, J.G., Päsler-Sauer, J., 1997. MET-RODOS: A Comprehensive Atmospheric Dispersion Module. Radiation Protection Dosimetry 73, 45–56.

Miller, M.E., 1967. Forecasting afternoon mixing depth's and transport wind speed. Monthly Weather Review 95, 35–44.

Monna, W.A.A., van der Vliet, J.G., 1987. Facilities for research and weather observations on the 213 m tower at Cabauw and at remote locations. De Bilt: KNMI Sci. Rep. WR 87–5, 27 pp.

Nieuwstadt, F.T.M., 1981. The steady state height and resistance laws of the nocturnal boundary layer: theory compared with Cabauw observations. Boundary-Layer Meteorology 20, 3–17.

Nieuwstadt, F.T.M., 1984. Some aspects of the turbulent stable boundary layer. Boundary-Layer Meteorology 30, 31–55.

Nieuwstadt, F.T.M., Driedonks, A.G.M., 1979. The nocturnal boundary layer – a case study compared with model calculations. Journal of Applied Meteorology 18, 1397–1405.

Noonkester, V.R., 1976. The evolution of the clear air convective layer revealed by surface based remote sensors. Journal of Applied Meteorology 15, 594–606.

Olesen, H.R., Jensen, A.B., Brown, N., 1987. An operational procedure for mixing height estimation. Risø National Laboratory MST-Luft-A96. 2nd edition 1992, 182 pp.

Overland, J.E., Davidson, K.L., 1992. Geostrophic drag coefficients over sea ice. Tellus 44A, 54–66.

Piringer, M., 1988. The determination of mixing heights by sodar in an urban environment. In: Grefen, K., Löbel, J. (Eds.), Environmental Meteorology. Kluwer Academic Publishers, Dordrecht, pp. 425–444.

Rao, K.S., Snodgrass, H.F., 1979. Some parameterizations of the nocturnal boundary layer. Boundary-Layer Meteorology 17, 41–55.

Rayner, K.N., Watson, D., 1991. Operational prediction of daytime mixed layer heights for dispersion modeling. Atmospheric Environment 25A, 1427–1436.

Russell, P.B., Uthe, E.E., Ludwig, F.L., Shaw, N.A., 1974. A comparison of atmospheric structure as observed with monostatic acoustic sounder and lidar techniques. Journal of Geophysical Research 79, 5555–5566.

San José, R., Casanova, J., 1988. An empirical method to evaluate the height of the convective boundary layer by using small mast measurements. Atmospheric Research 22, 265–273.

Schlünzen, K.H., 1994. Mesoscale modelling in complex terrain – an overview on the German nonhydrostatic models. Contributions to Atmospheric Physics 67, 243–253.

Seibert, P., Beyrich, F., Gryning, S.E., Joffre, S., Rasmussen, A., Tercier, P., 1998. Mixing layer depth determination for dispersion modelling. European Commission. In: Fisher, B.E.A., Erbrink, J.J., Finardi, S., Jeannet, P., Joffre, S., Morselli, M.G., Pechinger, U., Seibert, P., Thomson, D.J. (Eds.), 1998: COST Action 710-Final Report. Harmonisation of the pre-processing of meteorological data for atmospheric dispersion models. L-2985 Luxembourg: European Commission, EUR 18195 EN (ISBN 92-828-3302-X).

Servizi Territorio, 1994. PBL_MET, a software library for advanced meteorological and air quality data processing. Cinisello Balsamo, Italy.

Smedman, A.S., 1988. Observations of multi-level turbulence structure in a very stable atmospheric boundary layer. Boundary-Layer Meteorology 44, 231–253.

Smedman, A.S., 1991. Some turbulence characteristics in stable atmospheric boundary layer flow. Journal of the Atmospheric Sciences 48, 856–868.

Sørensen, J.H., 1998. Sensitivity of the DERMA long-range Gaussian dispersion model to meteorological input and diffusion parameters. Atmospheric Environment 32, 4195–4206.

Sørensen, J.H., Rasmussen, A., Svensmark, H., 1996. Forecast of atmospheric boundary layer height utilised for ETEX real-time dispersion modelling. Physics and Chemistry of the Earth 21, 435–439.

Sørensen, J.H., Rasmussen, A., Ellermann, T., Lyck, E., 1998. Mesoscale influence on long-range transport, evidence from ETEX modelling and observations. Atmospheric Environment 32, 4207–4217.

Steyn, D.G., 1990. An advective mixed layer model for heat and moisture incorporating an analytic expression for moisture entrainment. Boundary-Layer Meteorology 53, 21–31.

Stull, R.B., 1976a. The energetics of entrainment across a density interface. Journal of the Atmospheric Sciences 33, 1260–1267.

Stull, R.B., 1976b. Internal gravity waves generated by penetrative convection. Journal of the Atmospheric Sciences 33, 1279–1286.

Stull, R.B., 1983a. A heat flux history length scale for the nocturnal boundary layer. Tellus 35A, 219–230.

Stull, R.B., 1983b. Integral scales for the nocturnal boundary layer. Part I: Empirical depth relationships. Journal of Climate Applied Meteorology 22, 673–686.

Stull, R.B., 1988. An Introduction to Boundary Layer Meteorology. Kluwer Academic Publishers, Dordrecht, 665 pp.

Tennekes, H., 1970. Free convection in the turbulent Ekman-layer of the atmosphere. Journal of the Atmospheric Sciences 27, 1027–1033.

Tennekes, H., 1973. A model for the dynamics of the inversion above a convective boundary layer. Journal of the Atmospheric Sciences 30, 558–567.

Tennekes, H., van Ulden, A.P., 1974. Short term forecasts of temperature and mixing height on sunny days. Proceedings of Second AMS Symposium Atmospheric Diffusion & Air Pollution, Santa Barbara, pp. 35–40.

Tercier, Ph., Stübi, R., Häberli, Ch., 1995. Evaluation de la hauteur de la couche limite de mélange dans le cadre du projet POLLUMET. Report of the Swiss Meteorol. Inst., 31 pp.

Tjemkes, S.A., Duynkerke, P.G., 1989. The nocturnal boundary layer: Model calculations compared with observations. Journal of Applied Meteorology 28, 161–175.

Troen, I., Mahrt, L., 1986. A simple model of the planetary boundary layer: Sensitivity to surface evaporation. Boundary-Layer Meteorology 37, 129–148.

van Pul, W.A.J., Holtslag, A.A.M., Swart, D.P.J., 1994. A comparison of ABL-heights inferred routinely from lidar and radiosonde at noontime. Boundary-Layer Meteorology 68, 173–191.

Vogelezang, D.H.P., Holtslag, A.A.M., 1996. Evolution and model impacts of alternative boundary layer formulations. Boundary-Layer Meteorology 81, 245–269.

Weil, J.C., Brower, R.P., 1983. Estimating convective boundary layer parameters for diffusion applications. Report PPSP-MP-48. Prepared by Environmental Center, Martin Marietta Corporation, for Maryland Department of Natural Resources, Annapolis, MD.

Wetzel, P.J., 1982. Toward parameterization of the stable boundary layer. Journal of Applied Meteorology 21, 7–13.

Wotawa, G., Stohl, A., Kromp-Kolb, H., 1996. Parameterization of the planetary boundary layer over Europe: A data comparison between the observation-based OML preprocessor and ECMWF model data. Contributions to Atmospheric Physics 69, 273–284.

Wyngaard, J.C., 1975. Modeling the planetary boundary layer – extension to the stable case. Boundary-Layer Meteorology 9, 441–460.

Yamada, T., Berman, S., 1979. A critical evaluation of a simple mixed layer model with penetrative convection. Journal of Applied Meteorology 18, 781–786.

Yu, T.W., 1978. Determining the height of the nocturnal boundary layer. Journal of Applied Meteorology 17, 28–33.

Zeman, O., Tennekes, H., 1977. Parameterization of the turbulent kinetic energy budget at the top of the daytime boundary layer. Journal of the Atmospheric Sciences 34, 111–123.

Zilitinkevich, S.S., 1972. On the determination of the height of the Ekman boundary layer. Boundary-Layer Meteorology 3, 141–145.

Zilitinkevich, S.S., 1975. Comments on a paper by H. Tennekes. Journal of the Atmospheric Sciences 32, 991–992.

Zilitinkevich, S.S., Fedorovich, E.E., Shabalova, M.V., 1992. Numerical model of a non-steady atmospheric planetary boundary layer, based on similarity theory. Boundary-Layer Meteorology 59, 387–411.

Zilitinkevich, S.S., Mironov, D.V., 1996. A multi-limit formulation for the equilibrium depth of a stably stratified boundary layer. Boundary-Layer Meteorology 81, 325–351.